Published in final edited form as:

Cell. 2019 February 21; 176(5): 1190–1205.e20. doi:10.1016/j.cell.2018.12.041.

Limbic neurons shape sex recognition and social behavior in sexually naïve males

Daniel W. Bayless[1], **Taehong Yang**[1], **Matthew M. Mason**[1], **Albert A.T. Susanto**[1], **Alexandra Lobdell**[1], and **Nirao M. Shah**[1,2,3,*]

[1]Dept. of Psychiatry and Behavioral Sciences, Stanford University, Stanford, CA 94305, USA

[2]Dept. of Neurobiology, Stanford University, Stanford, CA 94305, USA

[3]Lead Contact

SUMMARY

Sexually naïve animals have to distinguish between the sexes because they show species-typical interactions with males and females without meaningful prior experience. However, central neural pathways in naïve mammals that recognize sex of other individuals remain poorly characterized. We examined the role of the principal component of the bed nucleus of stria terminalis (BNSTpr), a limbic center, in social interactions in mice. We find that activity of aromatase-expressing BNSTpr (AB) neurons appears to encode sex of other animals and subsequent displays of mating in sexually naïve males. Silencing these neurons in males eliminates preference for female pheromones and abrogates mating success, whereas activating them even transiently promotes male-male mating. Surprisingly, female AB neurons do not appear to control sex recognition, mating, or maternal aggression. In summary, AB neurons represent sex of other animals and govern ensuing social behaviors in sexually naïve males.

Grapical Abstarct

*Correspondence: nirao@stanford.edu.

AUTHOR CONTRIBUTIONS

Conceptualization, DWB and NMS; Funding, NMS; Investigation, AATS, AL, DWB, MMM, and TY; Supervision, DWB and NMS; Writing, DWB and NMS.

DECLARATION OF INTERESTS

The authors declare no competing interests.

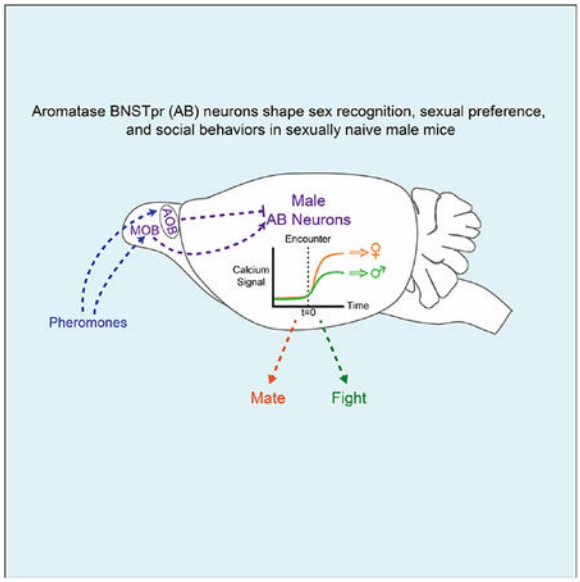

Aromatase-expressing BNSTpr neurons govern sex recognition, sexual preference, mating, and aggression in sexually naïve males, and their activation is sufficient to promote male-male sexual behavior.

Aromatase-expressing BNSTpr neurons govern sex recognition and social behavior in naive male mice

INTRODUCTION

Sexually reproducing animals display sex differences in social behaviors that enhance reproductive success. Many sexually dimorphic behaviors are acquired traits, but others, such as mating or aggression, are innate in that they can be displayed without prior experience. Such primal interactions are guided by the sex of interacting individuals, indicating that naïve animals recognize the sex of their conspecifics. Indeed, naïve male mice mate with females but attack males. Neurons in the medial amygdala (MeA) and ventrolateral part of ventromedial hypothalamus (VMHvl) govern these behaviors in male mice (Hong et al., 2014; Lee et al., 2014; Unger et al., 2015; Yang et al., 2013, 2017; Yao et al., 2017), but only reliably code for sex following experience with females (Li et al., 2017; Remedios et al., 2017). Thus, other neurons must recognize the sex of conspecifics in naïve mice.

The BNSTpr (also referred to as BNSTmpm) expresses genes in a sexually dimorphic manner, including in humans, and Fos studies implicate it in social behaviors (Gammie and Nelson, 2001; Pfaus and Heeb, 1997; Ramos and DeBold, 2000; Shah et al., 2004; Stack et al., 2002; Wersinger et al., 1997; Wu et al., 2009; Xu et al., 2012; Yang et al., 2013; Zhou et al., 1995). BNSTpr neurons are juxtaposed with other functionally and molecularly heterogeneous BNST subnuclei that can also be sex hormone sensitive, and they are embedded in neural pathways underlying sexually dimorphic behaviors, including the MeA, VMHvl, and preoptic hypothalamus (POA) (Cooke and Simerly, 2005; Crestani et al., 2013;

Dong and Swanson, 2004; Giardino et al., 2018; Gu et al., 2003; Guillamón et al., 1988; Moga et al., 1989; Nelson and Trainor, 2007; Segovia and Guillamón, 1993; Simerly, 2002; Swanson, 2000; Walker et al., 2003; Zardetto-Smith et al., 1994). In mice and other animals, BNSTpr neurons are innervated by accessory olfactory bulb (AOB) neurons and are therefore one synapse away from neurons in the vomeronasal organ (VNO) (Broadwell, 1975; von Campenhausen and Mori, 2000; Davis et al., 1978). VNO neurons detect volatile and non-volatile pheromones, chemosensory cues that signal sexual, social, or reproductive status of an animal to other conspecifics (Chamero et al., 2007; Isogai et al., 2011; Kimoto et al., 2005; Liberles, 2014; Trinh and Storm, 2003). Finally, BNST lesions lead to deficits in sexual behavior in male rodents (Claro et al., 1995; Emery and Sachs, 1976; Lehman et al., 1983; Liu et al., 1997; Powers et al., 1987; Valcourt and Sachs, 1979). Despite these advances, the specific functions of BNSTpr neurons in social behaviors remain unclear because of a lack of markers that enable targeted studies of these cells.

Aromatase, which converts androgens to estrogens, is restricted to a subset of BNSTpr neurons in the mouse BNST (Fisher et al., 1998; Lephart, 1996; Naftolin et al., 1971; Wu et al., 2009). Both aromatase and estrogens are essential for development and functioning of sexually dimorphic social behaviors in the two sexes (Arnold, 2009; Honda et al., 1998; Matsumoto et al., 2003; McCarthy, 2008; Toda et al., 2001; Yang and Shah, 2014). We used genetically engineered mice to test the role of AB neurons in sexually dimorphic social behaviors. Calcium imaging of AB neurons in sexually naïve males revealed that these cells are differentially activated by males and females. Functional manipulations reveal that these neurons are necessary to distinguish the sexes and for ensuing social interactions, and that their activation elicits male-male mating. By contrast, female AB neurons appear not to participate in sex recognition or social interactions. Together, AB neurons represent a central neural locus for sex recognition in sexually naïve males to direct innate sex specific social behaviors.

RESULTS

AB neurons are active transiently in aggressive encounters

To image activity of AB neurons, we expressed a virally-encoded Cre-dependent calcium sensor GCaMP6s in AB neurons in $Aro^{Cre/IPIN}$ mice to perform fiber photometry (Chen et al., 2015; Cui et al., 2013; Gunaydin et al., 2014) (Figures 1A,B, S1A–C). $Aro^{Cre/IPIN}$ mice harbor *Cre* and *nuclear LacZ* in the 3'UTR of *aromatase* and enable manipulation of aromatase+ cells in behaviorally and physiologically wildtype (WT) mice (Unger et al., 2015; Wu et al., 2009). We confirmed functional expression of GCaMP6s in AB neurons in slices (Figure S1A–C). Next, we singly housed sexually naïve $Aro^{Cre/IPIN}$ males and imaged GCaMP6s fluorescence after inserting a WT male intruder. GCaMP6s signal increased with intruder entry and subsided after initial exploration of the intruder (69.1±11.7s to return to baseline, mean±SEM, n = 7) (Figure 1C,D,F; Movie S1). Following early exploration, resident males sniff (anogenital chemoinvestigation), tail rattle, or attack the intruder (Scott, 1966; Unger et al., 2015). We did not detect changes in GCaMP6s signal during these behaviors (Figure 1E–G; Figure S1F–H; Movie S1) (peak Fn during tail rattles: 1.01±0.002, p=0.34, n = 7). GCaMP6s lacks high temporal resolution and it is possible that baseline

firing of AB neurons is higher during an encounter with an intruder than single housing. Nevertheless, baseline fluorescence ($p = 0.41$, $n = 7$) was comparable between these two settings. A recent study reported that sexually naïve resident males do not attack intruder males (Remedios et al., 2017). By contrast, sexually naïve $Aro^{Cre/IPIN}$ resident males clearly attack intruder males, consistent with prior work and our tests with WT males (Figures 1G, S1I–N) (Connor, 1972; Crawley et al., 1975; King, 1957; Leypold et al., 2002; Maruniak et al., 1986; Stowers et al., 2002; Takahashi and Miczek, 2013; Yang et al., 2017). Technical differences in this recent study (Remedios et al., 2017) may have altered WT male behavior. Together, our findings show that sexually naïve males attack males, and that male AB neurons are active early in an encounter with males but not during attacks.

Females do not attack adults unless they are nursing (Gandelman, 1972), when they display maternal aggression and attack intruders. We therefore imaged GCaMP6s fluorescence in AB neurons of $Aro^{Cre/IPIN}$ mothers (Figure S1O). Although females have ~30% fewer AB neurons than males (Wu et al., 2009), we easily detected increased activity of female AB neurons upon insertion of intruders of either sex (Figure 1H–Q; Movie S1). Similar to resident males (Figure 1E,F), GCaMP6s signal did not change when mothers attacked or sniffed intruders (Figures 1J,K,O,P, S1P–U; Movie S1) or even when they retrieved their pups (Figure S1V-A'). In summary, AB neurons are active early in an agonistic encounter in resident males and mothers but not during attacks.

Mating activates male AB neurons

We imaged AB neurons in singly housed sexually naïve $Aro^{Cre/IPIN}$ males during mating with a WT sexually receptive female (Figures 2A, S2A). GCaMP6s signal increased upon entry of the female and subsided to baseline after initial exploration (97.7±10.5s, $n = 7$) (Figure 2B,F; Movie S2). Following early exploration, males display bouts of sniffing, mounting, and intromission (penetration) that can result in ejaculation (Figures 2G, S2D). AB neurons responded to mounts, intromission, and ejaculation, but not sniffing (Figure 2C–F; Figure S2B,C; Movie S2), indicating that they are active in many but not all interactions with females.

We also imaged AB neurons in singly housed, sexually naïve, receptive $Aro^{Cre/IPIN}$ females that were inserted into a WT male's cage (Figure S2E). Surprisingly, these cells were not activated during these interactions (Figure 2H–N; Figure S2F–K; Movie S2). These cells also did not respond appreciably during interactions with a WT receptive female that was inserted into their cage (Figure S2L–N). Female BNSTpr neurons are thought to be active during mating (Pfaus and Heeb, 1997). AB neurons are a subset of the BNSTpr (Wu et al., 2009), suggesting that, in females, aromatase–BNSTpr neurons are active during mating. We do not have a mouse line to image just the entire BNSTpr or aromatase–BNSTpr neurons. Most BNSTpr neurons and neighboring BNST subnuclei are GABAergic (Figure S2O–S) (Ng et al., 2009). We therefore imaged GABAergic BNST neurons in receptive $Vgat^{Cre}$ females (Vong et al., 2011) mating with WT males and found that these cells were activated during these interactions (Figure S2T–X; Movie S2). Thus we can detect activation of AB neurons in receptive females, thereby excluding technical issues with fiber photometry in this context. Although sexual experience increases female receptivity (Thompson and

Edwards, 1971; Xu et al., 2012), Vgat+ BNST neurons were active during mating in sexually naïve females. Thus, lack of sexual experience is unlikely to underlie the lack of detectable activity in AB neurons during mating. In summary, AB neurons are active during male but not female mating behavior.

Activity of AB neurons in sexually naïve males distinguishes between the sexes

The activity of male AB neurons appeared larger upon entry of a female than a male intruder (Figures 1D, 2B). To test this directly in individual males, we imaged AB neurons in singly housed, sexually naïve $Aro^{Cre/IPIN}$ males with intruders of both sexes (Figure 3A, S3A). AB neurons were specifically activated more upon entry of a female than a male regardless of the order of entry of intruders (Figure 3B–E). This sex-typical response reflects neither absolute differences in early interactions with the two sexes (Figure S3B,C) nor experience in mating or fighting because these behaviors were not observed in this brief 3 min test. Whether the same subset of AB neurons responds to the two sexes will entail probing these cells with single cell RNA-seq combined with functional studies. Importantly, AB neurons in sexually experienced males also responded more to females than males (Figure 3F,G; Figure S3E), indicating that mating does not alter AB neuronal responses to the two sexes.

These results suggest that male AB neurons encode or relay information relating to sex of conspecifics. Alternatively, they might encode motor drive or motivation to mate or fight. To distinguish between these models, we imaged AB neurons of sexually naïve resident males during 3 min encounters with male or female intruders before and after castrating (Cx) the residents (Figures 3H, S3F,G). AB neuron responses were comparable between pre-Cx and Cx males (Figure 3H,I). Cx males did not mate (0/4) with WT receptive females in 30 min assays, confirming functional absence of testosterone. Thus, male AB neurons respond differentially to the two sexes even when males do not mate or fight, indicating that the sex-typical response of these cells corresponds to sex recognition rather than purely motivational states or motor drives for social behaviors.

Mice use pheromones to distinguish the sexes (Baum and Bakker, 2013; Leypold et al., 2002; Stowers et al., 2002), suggesting that the early sex-typical response of AB neurons was elicited by intruder pheromones. We tested whether urine, a source of pheromones that can signal conspecific sex (Fu et al., 2015; Haga-Yamanaka et al., 2014; He et al., 2008; Holy et al., 2000; Kimoto et al., 2007; Meeks et al., 2010; Nodari et al., 2008; Tolokh et al., 2013), activated AB neurons. We imaged AB cells of sexually naïve $Aro^{Cre/IPIN}$ males after inserting cotton swabs wetted with male or female urine or saline (Figure 3J, S3D). AB neurons responded more to urine than to saline and more to female than male urine (Figure 3K–N; Movie S3). This response was smaller compared to insertion of mice (Figure 3A–C), suggesting that other cues also activate AB neurons. Unlike AB neurons, VNO neurons can respond in a binary manner to male or female urine (Holy et al., 2000). AOB mitral neurons, which are postsynaptic to VNO neurons, also show complex responses to the two sexes (Luo et al., 2003), suggesting significant transformation of sex recognition signals downstream of the VNO. Importantly, AB neurons did not respond to 2-phenylethylamine (PEA) or cadaverine, cues found in predator urine and decomposing tissue respectively (Ferrero et al.,

2011; Liberles, 2014, 2015) (Figure S3H–J). Thus, AB neurons respond selectively and differentially to pheromones from male and female conspecifics.

Male mice prefer sniffing female to male urine (Baum and Bakker, 2013; Mandiyan et al., 2005; Pankevich et al., 2004; Yao et al., 2017), and we tested if disrupting AB neurons would alter this preference (Figure 3O). We silenced AB neurons of sexually naïve males with an inhibitory DREADD (DREADDi) and found that this abolished preference for female urine (Sternson and Roth, 2014) (Figures 3P, S3K–Q). The total time spent sniffing urine was unaltered (Figure 3Q), indicating that inhibiting AB cells does not disrupt the drive to chemoinvestigate objects. Acute manipulation of neuronal activity can disrupt systemic network function (Südhof, 2015) so we disrupted AB neurons with a complementary approach. We expressed in male AB neurons a designer caspase that leads to Cre-dependent autonomous apoptosis (Morgan et al., 2014; Yang et al., 2013) and found that ablation of AB cells also abolished preference for female urine (Figures 3R,S, S3R,S). In contrast to our photometry findings in males, AB neurons in mothers responded similarly to male and female intruders or insertion of male or female urine wetted swabs (Figure S3T-C'). In summary, male AB neurons provide information about intruder sex and regulate innate preference for female pheromones.

Male AB neurons require vomeronasal pheromone sensing to distinguish between the sexes

Male and female pheromones are sensed by distinct VNO neurons and AOB mitral cells (Ben-Shaul et al., 2010; Hammen et al., 2014; Holy, 2018; Luo et al., 2003). AOB mitral cells project to the BNSTpr (Broadwell, 1975; von Campenhausen and Mori, 2000; Davis et al., 1978), suggesting that this pathway drives the pheromone-elicited response of AB neurons. Indeed, Fos studies suggest a role for the VNO in activating BNSTpr (Halem et al., 1999; Pankevich et al., 2006). We first tested whether VNO pheromone sensing guided male preference for female urine. The cation channel Trpc2 is critical for VNO pheromone transduction, and $Trpc2^{-/-}$ males do not distinguish between the sexes (Leypold et al., 2002; Stowers et al., 2002). Although Trpc2 is expressed in some main olfactory epithelium (MOE) neurons, it's function in MOE neurons is unclear (Omura and Mombaerts, 2014). In any event, $Trpc2^{-/-}$ males did not show a preference for female urine (Figure 4A–C). We next imaged AB neurons in sexually naïve $Aro^{Cre/IPIN};Trpc2^{-/-}$ males and found that they responded similarly to urine from both sexes (Figures 4D–G, S4A). They also responded specifically and similarly to entry of a female or male intruder in a 3 min assay that precluded mating or aggression (Figure 4H–K). Activity of AB neurons upon presentation of female urine or intruder was comparable between $Aro^{Cre/IPIN}$ and $Aro^{Cre/IPIN};Trpc2^{-/-}$ males (peak Fn for female urine: $Aro^{Cre/IPIN}$ = 1.16±0.02, n = 10, and $Aro^{Cre/IPIN};Trpc2^{-/-}$ = 1.18±0.02, n = 5, p = 0.44; peak Fn for female intruder: $Aro^{Cre/IPIN}$ = 1.23±0.02, n = 14, and $Aro^{Cre/IPIN};Trpc2^{-/-}$ = 1.24±0.03, n = 5, p = 0.77) (Figures 3C,L, 4F,J). By contrast, their activity was larger upon presentation of male urine or intruder in $Aro^{Cre/IPIN};Trpc2^{-/-}$ males than $Aro^{Cre/IPIN}$ males (peak Fn for male urine: $Aro^{Cre/IPIN}$ = 1.08±0.02, n = 10, and $Aro^{Cre/IPIN};Trpc2^{-/-}$ = 1.18±0.02, n = 5, p = 0.0015; peak Fn for male intruder: $Aro^{Cre/IPIN}$ = 1.14±0.01, n = 14, and $Aro^{Cre/IPIN};Trpc2^{-/-}$ = 1.26±0.03, n = 5, p = 0.0003) (Figures 3C,L, 4F,J). Although it is difficult to compare GCaMP6s signal across different animal

cohorts, our findings indicate that loss of Trpc2 function increases the response of AB neurons to male pheromones. VNO neurons can detect volatile cues, but at least some of the response of AB neurons to volatile cues likely reflects input from pathways that relay MOE-initiated pheromonal signaling (Brennan et al., 1999; Kang et al., 2009, 2011a, 2011b; O'Connell and Meredith, 1984; Sam et al., 2001; Trinh and Storm, 2003).

VNO and mitral neurons are excitatory, but Trpc2-dependent signaling decreases response of male AB neurons to male pheromones. This may reflect developmental differences in Trpc2 mutants. Alternatively, pheromones excite or inhibit different AOB mitral cells in vivo (Luo et al., 2003), and disinhibition of these cells in Trpc2 mutants may elevate the response of AB neurons to male pheromones. The inhibitory influence of Trpc2-dependent signaling on AB neurons could also arise from network interactions locally or elsewhere. In any event, the differential response of male AB neurons to males and females relies on Trpc2-dependent pheromone transduction.

Trpc2$^{-/-}$ males mate with both sexes, and in longer assays (30 min), male AB neurons of *Aro*$^{Cre/IPIN}$;*Trpc2*$^{-/-}$ males were active during mating with either sex (Figure S4B–M; Movie S4). Males do not intromit or ejaculate when mating with males (Figure S4M), and the activity of AB neurons declined following a mount with a male (Figure S4D–H,K–M). However, peak GCaMP6s signal was comparable during mounts with either sex (peak Fn during mount: with female = 1.31±0.03, and with male = 1.26±0.02, n = 5, p =0.3359; Figure S4D,G,K,L). Thus, male AB neurons likely encode or relay information about the sex of conspecifics and regulate preference for female urine in a VNO-dependent manner.

AB neurons regulate male sexual behavior

Male AB neurons are active during mating so we tested whether they were required for this behavior. Chemogenetic inhibition of AB neurons of sexually naïve males profoundly reduced mating with a WT receptive female (Figures 5A–C, S5A). Most males did not mount or intromit, and none ejaculated, demonstrating a role of AB neurons in mating success. We did not find pervasive deficits in behavior (Figures 5B,C, S5B–G) or aggressive displays (0/14 males attacked females). These deficits were also observed in sexually naïve males in whom we ablated AB neurons (Figures 5D–F, S5H–L). These males in fact mounted less and did not intromit (Figure 5E,F), suggesting that DREADDi inhibition may have incompletely eliminated AB neuronal function. Female AB neurons are not active during sexual behavior (Figures 2H–N, S2I–K), and inhibition or ablation of these cells in *Aro*$^{Cre/IPIN}$ females did not alter receptivity or other behaviors (Figures 5G–N, S5M–W). In summary, AB neurons are required, both acutely and chronically, for WT levels of male mating.

AB neurons regulate male aggression

We next tested the males previously assayed with females (Figure 5A–F) with a WT male intruder. Both chemogenetic inhibition and ablation of AB neurons lowered the probability and reduced number of attacks without triggering mating (Figure 6A–F and Figures S5E, S6A,B). These findings suggest that the early response of AB neurons to males is critical for aggression. More generally, the diminution in aggression and mating following disruption of

male AB neurons suggests that inability to recognize males and females leads to a loss of meaningful interactions.

We next tested the role of AB neurons in maternal behavior. Neither chemogenetic inhibition nor targeted ablation of these cells led to detectable deficits in pup retrieval, maternal aggression, or other behaviors (Figures 6G–L, S6C–R). Ablation of AB neurons also did not alter litter size or percent pups surviving to weaning (Figure S6N–P). We cannot exclude incomplete functional disruption of female AB neurons, but we did observe behavioral deficits with similar manipulations in males. It is more likely that alternative neural pathways in the amygdala and hypothalamus are important for maternal care (Hashikawa et al., 2017; Unger et al., 2015). Thus, AB neurons appear to contribute minimally to maternal care but are critical for male aggression.

Persistent activation of male AB neurons promotes male-male mating

We wondered if optogenetic activation of male AB neurons would promote male mating. We expressed channelrhodopsin-2 (ChR2) (Fenno et al., 2011) in AB neurons of sexually naïve males and tested their behavior with WT male or receptive female intruders. Strikingly, laser illumination (473nm, 5Hz, 5ms pulse width, 30s cycles, 2mW) upon insertion of a male suppressed aggression and elicited mounting (Figure 7A–D, S7A,B,E–K; Movie S5). The few males (2/8) who attacked the intruder also mounted them. Mating attempts or attacks were not time-locked to laser illumination (Figure S7C), and the latency to initiate mounting toward the male was similar to male mating attempts with a female (Mount latency to females and males respectively, 447.1±82.1s and 365.3±90.7s, n = 5 females and 6 males, p = 0.5317; Figure 7D).

Activation of male AB neurons may not have triggered time-locked mating because intruder males are not receptive. However, optogenetic activation did not elicit time-locked mating with WT receptive females with the above (Figure S7D) or a different set of stimulation parameters (20Hz, 20ms pulse width, 30s cycles, 2mW; n=3). We also did not detect aberrant sexual behavior with females in that the latency to initiate and the number of various routines were unchanged (Figure 7E–H).

Optogenetic activation of AB neurons in receptive females did not alter their mating with WT males nor did it elicit male-type mounting (Table S1). Activating AB neurons in mothers also did not elicit male-type mating nor did it impair pup retrieval or aggression toward a male (Table S1). These findings complement the lack of a discernible behavioral phenotype after disrupting female AB neurons. Thus, activating AB neurons in males but not females inhibits aggression and biases the male to initiate mating toward males. In addition, the latency to mate with females is unchanged, indicating that early activation of male AB neurons upon encountering a female (Figures 2B,F, 3B,C,K,L) is salient and cannot be enhanced functionally by optogenetic activation.

Early activity of male AB neurons promotes mating

To test the relevance of early activity of male AB neurons, we used halorhodopsin (eNpHR3.0) to inhibit it in sexually naïve males (Fenno et al., 2011) (Figure S7L). We switched the laser on (593.5nm, 6mW), immediately inserted a WT receptive female, and

then switched the laser off after 90s, well before any mating attempts (0/8 males mounted a female in first 90s) (Figure 7I). This brief inhibition delayed the onset of mating 3-fold, reduced mounting, increased latency to intromit and ejaculate (Figure 7J–L), and did not elicit aggression (0/8 males attacked females). Similar to DREADDi inhibition and ablation studies, optogenetic inhibition for the entire test profoundly reduced male mating (Figures S7M–O, 5A–F). That males eventually mated after early transient inhibition suggests that they could subsequently process female cues that elicit this behavior. Together, these studies show that early activity of male AB neurons is critical for mating.

We next tested whether reducing laser power would elicit aggression toward receptive female intruders in a subset of these $Aro^{Cre/IPIN}$ males (5mW, 3mW, 1mW; n=3). Although more males mated with diminishing laser power (0/3, 1/3, 3/3 males mated at 5mW, 3mW, and 1mW, respectively), they never attacked females. This suggests that optogenetic parameters may need to be optimized further or that other pathways inhibit male aggression toward females. In summary, transient early inhibition of male AB neurons delays mating well beyond the duration of laser illumination, demonstrating an enduring influence of the early activity of AB neurons in mating.

Male AB neurons also respond early in intermale encounters, but this response is ~60% lower than the response to females (Figure 3C). We tested if enhancing this early activity would alter ensuing behavior with a male. We inserted a WT male and immediately activated ChR2+ AB neurons of the male residents for 90s (473nm, 5Hz, 5ms pulse width, 2mW) (Figure 7M, S7P), a period during which residents did not mate or fight (0/5 residents mated or fought). Strikingly, residents now attempted to mate with rather than attack male intruders (Figure 7N–P; Movie S5). This brief activation did not alter latency to sniff intruders, and the latency to initiate mating was similar to that observed when males mated with females (Figure 7P). We observed mount attempts even toward the end of the 15 min assay, demonstrating a perduring influence of the initial 90s of stimulation. It is unclear if these enduring behavioral changes reflect alterations in sex recognition or other internal states. Regardless, early activation of male AB neurons seems to provide a signal that induces a long-lasting change such that males functionally misidentify other males as females in the sense that they attempt to mate with them.

DISCUSSION

Naïve animals must innately distinguish between the sexes in order to engage in courtship or territorial displays. Neurons that reliably distinguish between males and females in sexually naïve mammals have remained elusive, and displays of innate behaviors such as aggression have even been proposed to require sexual experience (Remedios et al., 2017). Here we show that the activity of AB neurons distinguishes between the sexes in sexually naïve males. Together, our findings suggest that these cells are central to deciding the course of action during social encounters. Activity of AB neurons enables a male to distinguish between the sexes and enact a decision to mate with females and attack males. In this model, disrupting AB neurons precludes males from recognizing the sex of other animals, and virtually eliminates selection of either course of action, mating with females or attacking males.

Role of male AB neurons in social behaviors

The early response of male AB neurons that distinguishes the sex of intruders relies on Trpc2-dependent signaling, which is also critical to distinguish between the sexes (Leypold et al., 2002; Stowers et al., 2002). These neurons are unlikely to exclusively control motor drive or motivation to mate or fight because disrupting their function does not eliminate motivated behaviors, activating them does not elicit time-locked behavior, and they respond differentially to the two sexes in Cx males who do not mate or fight. Together, our findings suggest that male AB neurons encode Trpc2-dependent information about the sex of conspecifics that is critical for ensuing social behaviors.

Although male AB neurons are active during mating, experimental activation of these cells biases males to mate without eliciting discernible time-locked mating routines. Further optimization of stimulation parameters might elicit time-locked behaviors. Alternatively, activity of AB neurons during mating could reflect sensory input, internal states relating to mating, or an efference copy of motor programs. Surprisingly, AB neurons are active during the early but not later exploration of an intruder although exploration includes sniffing that enables access to pheromones. Early exploration may involve behaviors that are hard to detect, or the response of AB neurons to sniffing may be suppressed during later exploration.

Our studies suggest a model for why *Trpc2*$^{-/-}$ males mate with both sexes. The activity of male *Trpc2*$^{-/-}$ AB neurons mis-identifies males as females, leading to indiscriminate mating and a loss of fighting. The source of this signal is likely to be the MOE, because AB neurons respond to pheromones in *Trpc2*$^{-/-}$ males. Accordingly, disrupting AB neurons precludes relay of this MOE-derived signal and essentially abrogates mating and fighting, mirroring the phenotype of males with genetically disabled MOE function (Mandiyan et al., 2005; Wang et al., 2006; Yoon et al., 2005). Both the MOE and VNO regulate social behaviors (Keller et al., 2009), and our results show that male AB neurons shape sex recognition and social behaviors likely by processing signals from both MOE and VNO.

Sex differences in the function of AB neurons

We find that female AB neurons do not appear to recognize sex or contribute to behavioral output. The function of these cells may have been hard to discern in our assays or our perturbations may have been inadequate. Nevertheless, similar perturbations in males revealed important functions of AB neurons. More likely, the observed functional sex differences in AB neurons reflect dimorphisms in local or long distance circuit computation. In any event, the two sexes appear to employ dimorphic neural substrates to distinguish between and interact with males and females.

We have identified many differences between male and female AB neurons under sex-typical hormonal conditions. Whether these dimorphisms are developmentally hard-wired or reflect circulating hormones in adults (Becker et al., 2005) is unclear. Given the importance of aromatase in sexual differentiation and social behaviors, its function in AB neurons should be explored in future studies.

AB neurons distinguish between the sexes and enable social interactions in sexually naïve males

In contrast to male AB neurons, male MeA and VMHvl neurons reliably report sex of conspecifics only following experience with females (Li et al., 2017; Remedios et al., 2017), and stimulation of these (or POA) neurons elicits time-locked behaviors (Hong et al., 2014; Lee et al., 2014; Wei et al., 2018). Thus, the neural pathway underlying innate sex recognition may be distinct from that which regulates mating or fighting. This is analogous to models for parallel visual processing of "where" and "what" functions for object localization (Nassi and Callaway, 2009; Seabrook et al., 2017). Male AB neurons may encode "which sex" whereas MeA and VMHvl neurons may encode "how to act" with that sex. This model does not preclude cross-talk or additional distributive processing of social behaviors. Alternatively, a hierarchical pathway may underlie social behaviors such that AB neurons report biological sex to guide behavioral choice, and MeA, VMHvl, and POA neurons read out activity of AB neurons to enact distinct motor programs of social behavior.

Momentary activation of male AB neurons promotes a bias to mate rather than fight and appears to render ineffective incoming input about aggression-eliciting male cues. If sexual identification of individuals initiates a decision about how to interact with them, our findings show that this decision is reached quickly, enacted after a brief delay, and seems impervious to additional sensory evidence. It will be fascinating to understand mechanisms underlying this enduring cognitive state that guides social behaviors.

STAR*METHODS

CONTACT FOR REAGENT AND RESOURCE SHARING

Further information and requests for resources and reagents should be directed to and will be fulfilled by the Lead Contact, Nirao Shah (nirao@stanford.edu).

EXPERIMENTAL MODEL AND SUBJECT DETAILS

Mice—Animal studies were conducted following Institutional Animal Care and Use Committee guidelines and protocols. Adult mice 10–24 weeks of age were used for all studies. Mice were bred in our colony ($Aro^{Cre/IPIN}$, Aro^{IPIN}, $Trpc2^{-/-}$, $Vgat^{Cre}$, and $Gad1^{EGFP}$) (Leypold et al., 2002; Tamamaki et al., 2003; Unger et al., 2015; Vong et al., 2011; Wu et al., 2009) or purchased from Jackson (C57BL/6J for WT females), Taconic (129/SvEvTac for WT males), and Charles River (C57BL/6N for tests of WT sexually naïve inter-male aggression shown in Figure S1H–J). $Aro^{Cre/IPIN}$ mice harbor Cre recombinase and nuclear LacZ (Unger et al., 2015; Wu et al., 2009) inserted 3' of IRES elements separately into the 3'UTR of aromatase in a gene conserving manner. Mice were housed under a 12:12 hr light:dark cycle, and water and food were available *ad libitum* unless otherwise mentioned. Mice were group housed by sex after weaning at 3 weeks of age and were therefore sexually naïve prior to initiation of behavioral testing unless otherwise mentioned. Recent findings indicate that Swiss Webster (SW) females display maternal aggression more reliably than the C57BL/6J background in which $Aro^{Cre/IPIN}$ mice are maintained (Hashikawa et al., 2017). To test whether we would observe comparable or different phenotypes in females from this more aggressive strain, we backcrossed the

Aro$^{Cre/IPIN}$ alleles into the SW background >3 times and subsequently assayed cohorts of these females for all studies in which female C57BL/6J mice had also been tested. Indeed, we did observe more maternal aggression in SW compared to C57BL/6J females (Table S1). However, all significant differences observed were seen in both strains, and there were no differences in the effects of our functional manipulations between the strains; therefore, we have provided data for SW and C57BL/6J females separately in Table S1 and combined data from both strains for graphical presentation in the figures.

METHOD DETAILS

Viruses—AAV-Syn-flex-GCaMP6s, AAV-EF1α-flex-hChR2(H 134R):eYFP, AAV-EF1 α-flex-eNpHR3.0:eYFP, and AAV-CAG-flex-eGFP were purchased from the Penn Vector Core. AAV-EF1α-taCasp3-TEVp, AAV-EF1α-flex-hM4DGi:mCherry, AAV-EF1α-flex-mCherry, and AAV-EF1α-flex-eYFP were purchased from the UNC Vector Core or custom packaged by the UNC Vector Core with plasmid DNA from our stocks or purchased from Addgene. All virus titers were >10^{12} genomic copies/mL.

Stereotaxic surgery—Viruses were delivered into brains of male and female mice at 10–16 weeks of age as described previously (Yang et al., 2013). Viruses were injected into empirically determined coordinates for the BNSTpr (±0.85 mm mediolateral, −0.20 mm anteroposterior, and −4.30 mm dorsoventral relative to bregma). For fiber photometry studies, 0.8 μl of virus was injected unilaterally (counterbalanced for injections into left or right hemisphere across animals), and for all functional manipulation studies, 0.8 μl of virus was injected bilaterally. Following viral injection during the same surgery, mice used for fiber photometry and optogenetic manipulation studies were implanted with an optic fiber 0.5 mm dorsal to the viral injection into the BNSTpr such that the optic fiber was extra-cranially housed in a ceramic cannula. For optogenetic studies, optic fibers were implanted bilaterally over the BNSTpr. The cannula was secured to the skull using adhesive dental cement (Parkell Inc). In addition, female mice used for mating assays were ovariectomized during the stereotaxic surgery while the virus was being delivered. Following surgery, mice were allowed to recover individually over a heat pad and then returned to their home cages.

Histology—We confirmed expression of virally delivered genes in all experimental animals using previously published procedures (Yang et al., 2013). We consistently achieved reliable infection of AB neurons, and we did not observe infection of other brain areas expressing aromatase including the POA and MeA. For histological analysis following behavioral testing, mice were perfused with 4% paraformaldehyde (PFA) and brains were dissected and post-fixed in 4% PFA overnight. Brains were sectioned at 65μm using a vibrating microtome (Leica) and then immunolabeled as described previously (Yang et al., 2013). The primary antisera used were: sheep anti-GFP (Biorad; 1:2000), rat anti-RFP (Chromotek; 1:2000), chicken anti-β-galactosidase (Abcam; 1:3000), and rabbit anti-Fos (Calbiochem; 1:2000). The fluorophore conjugated secondary antisera used were: Alexa Fluor 488 donkey anti-sheep (Jackson ImmunoResearch; 1:300), Cy3 donkey anti-rat (Jackson ImmunoResearch; 1:800), Alexa Fluor 488 donkey anti-chicken (Jackson ImmunoResearch; 1:300), Cy3 donkey anti-chicken (Jackson ImmunoResearch; 1:800), Alexa Fluor 647 donkey anti-chicken (Jackson ImmunoResearch; 1:500), and Cy3 donkey

anti-rabbit (Jackson ImmunoResearch; 1:800). Sections were also counterstained with DAPI (0.2 μg/ml). Optic fiber placement above the BNSTpr was verified for all mice used in fiber photometry and optogenetic manipulation studies, and Fos induction by ChR2 was confirmed by immunostaining for Fos in mice perfused 1 hr after 5 min of laser illumination (473nm, 5Hz, 5ms pulse width, 30s cycles, 2mW). Immunolabeled sections were imaged via confocal microscopy (Zeiss) and quantified using Image J software as described previously (Unger et al., 2015; Wu et al., 2009).

Slice imaging

Acute slice preparation: Slices through the BNSTpr were prepared from male and female Aro^{Cre} mice in whom an AAV encoding Cre-dependent GCaMP6s or control eGFP had been delivered into the BNSTpr 4 weeks prior to slice preparation. Mice were euthanized, and brains were dissected out and sectioned at 300 μm in ice-cold oxygenated (95% O_2/5% CO_2) saline containing 26mM $NaHCO_3$, 1.25 mM NaH_2PO_4, 3 mM KCl, 10 mM glucose, 210 mM sucrose, 2 mM $CaCl_2$, 2 mM $MgCl_2$. Slices were then transferred to oxygenated artificial cerebrospinal fluid (aCSF) containing 125 mM NaCl, 25 mM $NaHCO_3$, 1.25 mM NaH_2PO_4, 4 mM KCl, 15 mM glucose, 2 mM $CaCl_2$ and 1 mM $MgCl_2$ and incubated at 34°C for 30 min.

Calcium imaging: Slices were moved to an imaging chamber containing aCSF positioned below a digital camera (ORCA-ER, Hamamatsu) mounted on an Olympus upright microscope (BX51WI). Micro-manager software (version 1.4) was used to control the microscope interface. Cells were imaged at 10× magnification (5 Hz; 200ms exposure time) with 470 nm excitation through a filter set (U-N41 017, E.X. 470 nm, B.S. 495 nm, E.M. 5, Olympus). Throughout the experiment, slices were superfused with oxygenated aCSF. Initially aCSF KCl concentration was set at physiological levels of 4mM. In order to measure the relationship between neuronal depolarization and changes in GCaMP6s fluorescence, aCSF KCl concentration was systematically increased to elicit increased neuronal depolarization. After an initial 5 min 4mM KCl baseline period, KCl concentration was increased to 10mM for 5 min, followed by 15mM for 5 min, and finally a return to 4mM baseline for 5 min.

Data analysis: Data analysis was performed as described previously (Chen et al., 2015). Individual regions of interest (ROIs) containing an identifiable cell nucleus were selected using the oval selection tool in ImageJ. Then, using the Plot Z-Axis Profile function in Image J, the mean gray value of each ROI was obtained for all frames ($F_{Cell\_Measured}$). Additionally, an estimate of neuropil fluorescence ($F_{Neuropil}$) was obtained by selecting the surrounding of the cell using the same procedures. The true fluorescence signal of each cell was then estimated using the function: $F_{Cell\_True(t)} = F_{Cell\_Measured(t)} - (F_{Neuropil(t)} \times r)$, with $r = 0.7$ (Chen et al., 2015). $F_{Cell\_True(t)}$ for each cell was then normalized to the median of the initial 5 min 4mM KCl baseline period. To establish the relationship between neuronal depolarization and GCaMP6s fluorescence, peak Fn (see below) averaged across cells in the final minute of the four KCl concentration conditions was compared for male and female GCaMP6s and control eGFP groups.

Fiber Photometry

Calcium imaging: Fiber photometry was conducted as described previously (Chen et al., 2015; Cui et al., 2013; Gunaydin et al., 2014). Briefly, using a fiber photometry setup (Figure 1B), a 473 nm laser diode excitation source (Omicron Luxx) was placed upstream to an optic chopper (Thorlabs) running at 400 Hz and then passed through a GFP excitation filter (Thorlabs). This signal was then reflected by a dichroic mirror (Semrock) into an optic fiber cable (Thorlabs). This cable was then linked to an optic fiber implant attached to the experimental mouse. Fluorescence emitted by GCaMP6s during the behavioral assay was filtered through a GFP emission filter (Thorlabs) and focused by a convex lens (Thorlabs) onto a photoreceiver (Newport 2151). The signal was then run into a lock-in amplifier (Stanford Research System), digitized by a data acquisition device (LabJack U6-Pro), and recorded on a computer at a 250 Hz sampling rate.

Optic fibers and cannulas were made using multimode fiber with a 400 μm core (Thorlabs FP400URT) that was stripped with a fiber stripper, lightly scored by an optic fiber scribe (Thorlabs S90R), and pulled by hand to create an optic fiber of appropriate length for implantation. The pulled end of each optic fiber was then inspected using a fiber microscope (Thorlabs FS200) and only fibers with > 90% smooth surface were used. Optic fibers were then inserted into a 2.5 mm ceramic ferrule (Thorlabs CF440–10), and fiber epoxy (Thorlabs F112) was applied to both ends and allowed to cure overnight. Finally, optic fibers were polished using a polishing disk (Thorlabs D50-FC) and calcined alumina lapping sheets (Thorlabs LF03P).

Prior to any behavioral testing, mice were habituated to the weight and feel of the optic fiber cable. The cable was attached to the optic fiber implants on the mice, and mice were allowed to move freely in their home cages during 4 separate 30 min habituation sessions.

Data analysis: Behavioral video files and fluorescence data were time-locked via a light flash present in both datasets that was initiated by a pulse generator (Doric OTPG-4). The raw fluorescence data was normalized to the median fluorescence of the 5 min baseline period before the entrance of any animal or object into the cage. For PETP, time zero was set to the start of a behavior or event of interest, and the median fluorescence during the time window 10 s prior to a behavioral event was used as the normalization factor to calculate change in fluorescence from baseline (F_n). For peri-event analysis of amplitude changes, the 95 percent peak fluorescence (peak F_n) was calculated and compared for the 10 s time window before and after a behavioral event. For mounting behavior, which transitions into intromission within 2–4 s, the time window from the initiation of mounting up until the start of intromission was used to calculate 95 percent peak F_n.

Chemogenetic inhibition—Chemogenetic inhibition studies were performed as described previously (Unger et al., 2015; Yang et al., 2017). CNO (Enzo) was dissolved in sterile saline at 5 mg/ml and kept as frozen aliquots. On the day of behavioral testing, CNO was freshly diluted in sterile saline to achieve a dose of 1 mg/kg. This dose of CNO was optimized for our studies and falls within the range used in previous studies (Unger et al., 2015; Yang et al., 2017). Experimental mice were injected intraperitoneally (IP) with CNO

or sterile saline 30 min prior to behavioral assays. Mice were tested on each behavioral assay once each with CNO and saline, with the order of CNO and saline administration counterbalanced across animals.

Caspase-3 mediated ablation—Caspase-mediated ablation studies were performed as described previously (Unger et al., 2015; Yang et al., 2013). We virally expressed a Cre-dependent executioner caspase-3 in AB neurons in $Aro^{Cre/IPIN}$ and control Aro^{IPIN} mice, and waited ≥3 weeks to allow for maximal ablation of AB neurons. Only animals in which both the left and right BNSTpr showed cell loss >50% compared to the number of aromatase cells in control Aro^{IPIN} mice were included for behavioral scoring and analysis. Animals were tested twice for each behavioral assay with their behavioral performance averaged across both assays for data presentation and analysis.

Optogenetic manipulation—Optic fibers and cannulas were made as described above for fiber photometry but with multimode fiber with a 200 μm core (Thorlabs FT200EMT) and 1.25 mm ceramic ferrules (Thorlabs CFLC230–10). All optogenetic stimuli were produced by a pulse generator (Doric OTPG-4) that triggered a blue light laser for ChR2 studies (473 nm; Opto Engine) and a yellow light laser for eNpHR3.0 studies (593.5 nm; Opto Engine). Laser illumination commenced as soon as an intruder was placed into the residents cage. For ChR2 studies, laser power was adjusted such that light exiting the optic fiber cable was 2mW. For persistent photostimulation, laser illumination was performed in cycles of 30 s light on and 30 s light off throughout the entire assay. For transient photostimulation, laser illumination was done continuously at 5Hz for the first 90s of the assay, and then illumination was turned off for the rest of the assay. For eNpHR3.0 studies, laser power was adjusted such that light exiting the optic fiber cable was 6mW unless otherwise mentioned. For constant inhibition studies, laser illumination was on throughout the entire assay. For transient inhibition studies, laser illumination was continuously on for 90 s, and then illumination was switched off for the rest of the assay. For ChR2 and eNpHR3.0 studies, mice were tested on each assay once each with light illumination and no light illumination control, counterbalanced across animals. As with fiber photometry, prior to any behavioral testing, mice were habituated to the weight and feel of the optic fiber cable. Mice were given 4 separate 30 min habituation sessions.

Hormone priming—To control for cyclic hormone levels, all females used in mating assays were ovariectomized as described previously (Unger et al., 2015; Wu et al., 2009; Xu et al., 2012; Yang et al., 2013). To induce receptivity, females were hormonally primed by subcutaneous injection of 10 μg of 17-β-estradiol benzoate (EB, Sigma) suspended in sesame oil (48hrs before the assay), followed by 5 μg of EB (24hrs before the assay), and finally 50 μg of progesterone (Sigma) suspended in sesame oil (4–6hrs before the assay).

Hormone assays—Serum testosterone levels were measured using an ELISA kit (Cayman, #582701) (Yang et al., 2017) following the manufacturer's instructions.

Behavioral testing—All behavioral testing was initiated ≥ 1 hr after onset of the dark cycle and recorded using camcorders (Sony) under infrared illumination as described previously (Yang et al., 2013). Videos were played at 30 frames per second and manually

annotated using custom software described previously (Wu et al., 2009; Xu et al., 2012; Yang et al., 2013). This permitted analysis of multiple parameters (including number, duration, latency, probability, and inter-event interval) of different behavioral routines. In particular, anogenital investigation (sniff), mounting, repeated pelvic thrust (intromission), and ejaculation were scored for sexual behaviors. Receptivity index was calculated by dividing number of intromissions by number of mounts for each mouse. Lordosis events were defined by the display of a concave-arched back posture while braced on all four legs during a mount attempt. Lordosis Quotient (or Receptivity Quotient) was calculated as follows: (# lordosis events*100)/(# mounting events) (Thompson and Edwards, 1971). Aggression was scored as occurring when physical attacks (episodes of biting, wrestling, tumbling, chasing) were observed.

Both sexual and aggressive displays were annotated during female-male and male-male interactions. Mating assays during male-female interactions lasted for 30 min to enable display of different mating routines. Aggression assays (male-male; nursing female-intruder of either sex) were restricted to 15 min to allow fighting to occur but were short enough to preclude excessive attacks toward intruders. All behavioral studies were conducted using previously published procedures (Unger et al., 2015; Wu et al., 2009; Xu et al., 2012; Yang et al., 2013). The various behavioral assays used in the study are described briefly below.

Testing aggression in WT sexually naïve males: For testing aggression in C57Bl/6N males {the strain used in (Remedios et al., 2017)}, we purchased adult sexually naïve males who had been group housed since weaning from Charles River; upon receipt of these males, we acclimated them to our reverse light cycle (lights-on at 1PM and lights-off at 1AM) for 14 days in group housing condition. However, males to be used as residents were acclimated to the reverse light cycle for 7 days, singly housed for 7 days, and then tested with group housed intruders of the same strain.

Sequence of behaviors for Figures 1, 2: To examine male AB neuronal activity during social interactions, we targeted a virally-encoded Cre-dependent GCaMP6s to and implanted an optic fiber over AB neurons of sexually naïve $Aro^{Cre/IPIN}$ males that had been group housed by sex since weaning; we waited ≥4 weeks to allow for maximal viral expression. Prior to fiber photometry studies, these males were single housed for ≥ 7 days. Separate cohorts of males were assayed in their home cage during either a 15 min interaction with a WT group housed male or a 30 min interaction with a WT group housed hormonally primed female; for both of these cohorts, we assayed for changes in GCaMP6s fluorescence in multiple assays until the experimental male exhibited typical social displays, mating toward female intruder and aggression toward male intruder. Experimental males from both cohorts showed social behaviors even in the first assay (3/7 mated with females and 4/7 attacked males), and all males from both cohorts exhibited mating with females or aggression with males within 3 rounds of testing. Importantly, in no case was an experimental male being tested with an intruder of one sex ever tested with an intruder of the opposite sex; for example, none of the experimental males being tested with an intruder male underwent testing with a female, and they were therefore sexually naïve at the time of euthanasia unless otherwise mentioned.

To examine female AB neuronal activity during maternal behaviors, we targeted a virally-encoded Cre-dependent GCaMP6s to and implanted an optic fiber over AB neurons of sexually naïve *Aro*$^{Cre/IPIN}$ females that had been group housed by sex since weaning; we waited ≥4 weeks to allow for maximal viral expression. For assays of maternal behavior, a cohort of females was housed with WT male until visibly pregnant. Males were then removed (≥ 5 days prior to fiber photometry studies), and females were allowed to deliver their litter. To assay pup retrieval, at days 2 and 4 after parturition, all pups were briefly removed from the cage and 4 pups were placed separately in the corners of the cage. Pup retrieval behavior was assayed for 5 min, allowing sufficient time for mothers to retrieve all pups. Following the assay, all pups were returned to the cage. To assay maternal aggression, pups at postnatal day 6, 8, 10, and 12 were removed, and a WT group-housed male or hormonally primed female intruder was inserted into the cage for 15 min. The order of the sex of the intruder (days 6 and 8 vs days 10 and 12) was counterbalanced across mice. Pups were returned to the cage following completion of the assay. On postnatal day 14, pups were removed briefly, and females were exposed for 3 min to a novel object (1.25” cubed wood block). Finally, on postnatal days 16, 18, and 20, pups were removed from the cage, and females were exposed for 3 min to a 1”x1” cotton swab wetted with urine or saline as described below.

To examine female AB neuronal activity during sexual behavior (Figures 2, S2), we targeted a virally-encoded Cre-dependent GCaMP6s to and implanted an optic fiber over AB neurons of sexually naïve *Aro*$^{Cre/IPIN}$ or *Vgat*^{Cre} females that had been group housed by sex since weaning and removed their ovaries; we waited ≥4 weeks to allow for maximal viral expression. These females were single housed for ≥ 7 days prior to fiber photometry studies. To assay sexual behavior, these females were hormonally primed to be receptive and placed into the home cage of a WT sexually experienced male for 30 min. To examine the early response of sexually experienced estrus female AB neurons to the two sexes, these females were subsequently tested with group housed WT males or estrus females or wood block in 3 min encounters as described below for males.

Sequence of behaviors for Figure 3: To examine the early response of sexually naïve male AB neurons to the two sexes, we targeted a virally-encoded Cre-dependent GCaMP6s to and implanted an optic fiber over AB neurons of a new cohort of sexually naïve *Aro*$^{Cre/IPIN}$ males that had been group housed by sex since weaning; we waited ≥4 weeks to allow for maximal viral expression. Prior to fiber photometry studies, these males were single housed for ≥ 7 days. These males were exposed for 3 min on separate days in their home cage to a WT group housed hormonally primed receptive female, a WT group housed male, or wood block, with the order of the intruder assays counterbalanced across the 3 conditions.

To test whether sexual experience altered the response of AB neurons toward males and females, a subset of males used in the mating assays of Figure 2, which were now sexually experienced, were exposed for 3 min in their home cage, on separate days and in a counter-balanced manner, to a WT group housed male or receptive female intruder or novel object (wood block, 1.25” per side).

To test whether the loss of sexual motivation following Cx altered the response of AB neurons toward males and females, we expressed GCaMP6s as described in the next paragraph in another cohort of sexually naïve males and assayed them using the same 3 min encounter paradigm described above prior to and ≥14 days following Cx. Cx males of this latter cohort were subsequently tested for ≥30 min in their home cage with WT receptive females for male-typical mating behaviors to confirm functional absence of circulating testosterone prior to euthanasia.

To examine the early response of sexually naïve male AB neurons to pheromones or behaviorally salient odors, we expressed GCaMP6s in AB neurons as described above in another cohort of sexually naïve $Aro^{Cre/IPIN}$ males and exposed them for 3 min on separate days in their home cage to a 1”x1” cotton swab wetted with 80 μl of undiluted urine from WT group housed C57BL/6J males, primed receptive C57BL/6J females, or saline; the order of the swab assays was counterbalanced across the 3 conditions. Urine was collected 3–6 hours prior to use and kept on ice until pipetted onto the swab. To test the selectivity of the response of male AB neurons to specific odors, we expressed GCaMP6s in AB neurons as described above in a different cohort of sexually naïve $Aro^{Cre/IPIN}$ males and exposed them for 3 min on separate days in their home cage to cotton swabs wetted with 80 μL of 3μM PEA (Sigma) (Liberles, 2015), 20 μM cadaverine (Sigma) (Liberles, 2015), undiluted urine from males or females as described earlier in this paragraph, or saline in a counterbalanced manner. These males, who were still sexually naïve, were subsequently Cx and used as described in the preceding paragraph.

To test the effects of chemogenetic inhibition of male AB neuronal activity on pheromone preference, we targeted a virally-encoded Cre-dependent DREADDi (hM4DGi) to AB neurons of sexually naïve $Aro^{Cre/IPIN}$ males that had been group housed by sex since weaning; we waited ≥2 weeks to allow for maximal viral expression. Prior to pheromone preference assays, these males were single housed for ≥ 7 days. Males were tested on the pheromone preference assay once each with CNO and saline injected 30 min prior to the assay, with the order of CNO and saline administration counterbalanced across animals. During the preference assay, two 1”x1” cotton swabs (one wetted with 80 μl of undiluted WT group housed hormonally primed C57BL/6J female urine and the other wetted with 80 μl of undiluted WT group housed C57BL/6J male urine) were placed at opposite ends of their home cage. Mice were given 5 min to investigate the urine swabs. Duration, latency, and number of sniffs for each swab were scored. To test the effects of ablation of male AB neurons on pheromone preference, we targeted a virally-encoded Cre-dependent executioner caspase-3 to AB neurons of sexually naïve $Aro^{Cre/IPIN}$ and control Aro^{IPIN} males, and waited ≥3 weeks to allow for maximal ablation of AB neurons. Prior to pheromone preference assays, these males were single housed for ≥ 7 days. Males were then tested on the pheromone preference assay twice, and their performance was averaged across the two trials.

Sequence of behaviors for Figure 4: To examine the impact of Trpc2-dependent signaling on pheromone preference, we single housed $Trpc2^{-/-}$ and $Trpc2^{+/-}$ males for ≥ 7 days and subsequently tested them on the 5 min pheromone preference assay twice with their performance averaged across the two trials. To examine the impact of Trpc2-dependent

signaling on male AB neuronal activity, we targeted a virally-encoded Cre-dependent GCaMP6s to and implanted an optic fiber over AB neurons of sexually naïve $Aro^{Cre/IPIN}$; $Trpc2^{-/-}$ males that had been group housed by sex since weaning; we waited ≥4 weeks to allow for maximal viral expression. Prior to fiber photometry studies, these males were single housed for ≥ 7 days. These males were first assayed using the 3 min urine swab encounter paradigm described above and then subsequently assayed using the 3 min intruder encounter paradigm described above. Finally, these males were assayed in their home cage during separate 30 min interactions with a WT group housed male and a WT group housed hormonally primed receptive female.

Sequence of behaviors for Figure 5: To test the effects of chemogenetic inhibition of male AB neuronal activity on mating behavior, we targeted a virally-encoded Cre-dependent DREADDi to AB neurons of sexually naïve $Aro^{Cre/IPIN}$ males that had been group housed by sex since weaning; we waited ≥2 weeks to allow for maximal viral expression. Prior to mating assays, these males were single housed for ≥ 7 days. During the assay, a WT group-housed hormonally primed receptive female was inserted into the male's home cage for 30 min. Males were tested for mating behavior once each with CNO and saline injected 30 min prior to the assay, with the order of CNO and saline administration counterbalanced across animals. To test the effects of ablation of male AB neurons on mating behavior, we targeted a virally-encoded Cre-dependent executioner caspase-3 to AB neurons in $Aro^{Cre/IPIN}$ and control Aro^{IPIN} males, and waited ≥3 weeks to allow for maximal ablation of AB neurons. Prior to mating assays, these males were single housed for ≥ 7 days. Males were then tested on the 30 min mating assay twice with hormonally primed WT receptive females, and their performance was averaged across the two trials.

To test the effects of chemogenetic inhibition of female AB neuronal activity on sexual receptivity, we targeted a virally-encoded Cre-dependent DREADDi to AB neurons of sexually naïve $Aro^{Cre/IPIN}$ females that had been group housed by sex since weaning and removed their ovaries; we waited ≥2 weeks to allow for maximal viral expression. During the assay, group housed experimental females were hormonally primed to be receptive and then inserted into the home cage of a WT singly housed sexually experienced male for 30 min. Females were tested for sexual receptivity once each with CNO and saline injected 30 min prior to the assay, with the order of CNO and saline administration counterbalanced across animals. To test the effects of ablation of female AB neurons on sexual receptivity, we targeted a virally-encoded Cre-dependent executioner caspase-3 to AB neurons in $Aro^{Cre/IPIN}$ and control Aro^{IPIN} females, removed their ovaries, and waited ≥3 weeks to allow for maximal ablation of AB neurons. Group housed females were then tested on the 30 min sexual receptivity assay twice as described above, and their performance was averaged across the two trials.

Sequence of behaviors for Figure 6: To test the effects of chemogenetic inhibition of male AB neuronal activity on aggression behavior, experimental $Aro^{Cre/IPIN}$ males previously tested for mating behavior (Figure 5) were assayed for territorial aggression behavior. During the assay, a WT group-housed male was inserted into the experimental male's home cage for 15 min. Males were tested for aggression behavior once each with CNO and saline

injected 30 min prior to the assay, with the order of CNO and saline administration counterbalanced across animals. To test the effects of ablation of male AB neurons on aggression behavior, experimental $Aro^{Cre/IPIN}$ and control Aro^{IPIN} males previously tested for mating behavior (Figure 5) were assayed for territorial aggression behavior. Males were then tested on the 30 min territorial aggression assay twice, and their performance was averaged across the two trials.

To test the effects of chemogenetic inhibition of female AB neuronal activity on maternal behaviors, we targeted a virally-encoded Cre-dependent DREADDi to AB neurons of sexually naïve $Aro^{Cre/IPIN}$ females that had been group housed by sex since weaning; we waited ≥2 weeks to allow for maximal viral expression. These females were housed with WT male until visibly pregnant. Males were then removed (≥ 5 days prior to maternal behavior assays), and females were allowed to deliver their litter. Females were tested for each maternal behavior once each with CNO and saline injected 30 min prior to the assay, with the order of CNO and saline administration counterbalanced across animals. Pup retrieval assays as described above were conducted on days 3 and 5 after parturition. Percent retrieval, latency, and time to retrieve all pups were scored. On days 7 and 9 after parturition, pups were briefly removed from the cage, and a WT group housed male was inserted into the cage for 15 min. Following assays of maternal aggression, mothers were assayed for non-social behaviors. On days 11 and 13 after parturition, they were tested for anxiety-like behavior with the elevated plus maze. Females were placed in the center of an elevated plus maze facing the open arm at the start of the assay. Time spent in the closed or open arms during the 5 min assay was scored. On days 15 and 17 after parturition, females were tested for olfactory motivated behavior with a food finding assay. After being food deprived for 6hrs, females were inserted into a clean cage with a cracker (Cheez-It) buried under the bedding. Females were given 5 min to find the cracker at which time the assay ended. Latency to find the food was scored.

To test the effects of ablation of female AB neurons on maternal behaviors, we targeted a virally-encoded Cre-dependent executioner caspase-3 to AB neurons in $Aro^{Cre/IPIN}$ and control Aro^{IPIN} females, and waited ≥3 weeks to allow for maximal ablation of AB neurons. These females were housed with WT male until visibly pregnant. Males were then removed (≥ 5 days prior to maternal behavior assays), and females were allowed to deliver their litter. These females were then tested twice for the maternal behaviors described above in the same order and on the same post-natal days as with chemogenetic inhibition studies. Their performance was averaged across the two trials.

Following tests of mating and aggression, experimental males and females were also assayed for performance in elevated plus maze, latency to find hidden food, and locomotor activity as described above as well as previously (Unger et al., 2015; Xu et al., 2012; Yang et al., 2013). Furthermore, changes in body weight subsequent to ablation of AB neurons was assessed by weighing mice immediately prior to stereotaxic surgery and again prior to perfusion at the conclusion of the behavioral experiments. Mice were given ≥1 days between each behavioral test.

Sequence of behaviors for Figure 7: To test the effects of optogenetic activation of male AB neuronal activity on mating and aggression behavior, we targeted a virally-encoded Cre-dependent ChR2 to AB neurons of sexually naïve $Aro^{Cre/IPIN}$ males that had been group housed by sex since weaning and implanted optic fibers bilaterally over their BNSTpr; we waited ≥3 weeks to allow for maximal viral expression. Prior to behavioral assays, these males were single housed for ≥ 7 days. Males were tested, in a counter balanced order, on 30 min mating and 15 min aggression assays described above once each under light and no light conditions counterbalanced across animals. Laser illumination conditions are described above in the "Optogenetic manipulation" section. To test the effects of optogenetic activation of female AB neuronal activity on social interactions (Table S1), we targeted a virally-encoded Cre-dependent ChR2 to AB neurons of sexually naïve $Aro^{Cre/IPIN}$ females that had been group housed by sex since weaning, removed ovaries, implanted optic fibers bilaterally over their BNSTpr, and waited ≥3 weeks to allow for maximal viral expression. Prior to behavioral assays, these females were single housed for ≥ 7 days. Females were hormonally primed on the day of testing, and a WT group housed hormonally primed female was inserted into the cage for 30 min or the experimental females were inserted into the cage of WT sexually experienced male for 30 min in a counterbalanced manner. Females tested on the behavioral assay once each under persistent light and no light conditions counterbalanced across animals.

To test the effects of optogenetic inhibition of male AB neuronal activity on mating behavior, we targeted a virally-encoded Cre-dependent eNpHR3.0 to AB neurons of sexually naïve $Aro^{Cre/IPIN}$ males that had been group housed by sex since weaning and implanted optic fibers bilaterally over their BNSTpr; we waited ≥3 weeks to allow for maximal viral expression. Prior to behavioral assays, these males were single housed for ≥ 7 days. Males were tested on the 30 min mating assay described above once each under light and no light conditions counterbalanced across animals. Persistent and transient laser illumination conditions used are described above in the "Optogenetic manipulation" section unless mentioned otherwise.

QUANTIFICATION AND STATISTICAL ANALYSIS

Calcium imaging data, behavioral video recordings, and histological samples were analyzed blind to relevant variables, including sex, genotype, CNO administration, light illumination conditions, surgical procedure, and virus injected. Statistical analysis was performed using GraphPad PRISM (GraphPad Software). To compare categorical data including percentage of mice displaying a behavior, Fisher's exact test was performed from a 2×2 contingency table. To compare non-categorical data, including 95 percent peak F_n, duration of sniffing swabs and various behavioral parameters, we first determined if the data values were from a normal distribution using the D'Agostino-Pearson omnibus normality test. In experiments with paired samples, we used a paired t test or repeated measures ANOVA for parametric data and a Wilcoxon matched-pairs signed rank test or Friedman test for non-parametric data. In all other experiments, we used a t test or ANOVA for parametric data and a Mann-Whitney or Kruskal-Wallis test for non-parametric data. All multiple comparisons were corrected for using Bonferroni corrections.

Supplementary Material

Refer to Web version on PubMed Central for supplementary material.

ACKNOWLEDGMENTS

We thank Thomas Clandinin, Karl Deisseroth, Liqun Luo, Kristin Scott, Tom Südhof, and the Shah lab for discussions and Yiming Chen for input on photometry. This work was supported by grants from NIH (R01NS049488, R01NS083872) to NMS.

REFERENCES

Arnold AP (2009). The organizational-activational hypothesis as the foundation for a unified theory of sexual differentiation of all mammalian tissues. Horm Behav 55, 570–578. [PubMed: 19446073]

Baum MJ, and Bakker J (2013). Roles of sex and gonadal steroids in mammalian pheromonal communication. Frontiers in Neuroendocrinology 34, 268–284. [PubMed: 23872334]

Becker JB, Arnold AP, Berkley KJ, Blaustein JD, Eckel LA, Hampson E, Herman JP, Marts S, Sadee W, Steiner M, et al. (2005). Strategies and methods for research on sex differences in brain and behavior. Endocrinology 146, 1650–1673. [PubMed: 15618360]

Ben-Shaul Y, Katz LC, Mooney R, and Dulac C (2010). In vivo vomeronasal stimulation reveals sensory encoding of conspecific and allospecific cues by the mouse accessory olfactory bulb. Proc. Natl. Acad. Sci. U.S.A 107, 5172–5177. [PubMed: 20194746]

Brennan PA, Schellinck HM, and Keverne EB (1999). Patterns of expression of the immediate-early gene egr-1 in the accessory olfactory bulb of female mice exposed to pheromonal constituents of male urine. Neuroscience 90, 1463–1470. [PubMed: 10338312]

Broadwell RD (1975). Olfactory relationships of the telencephalon and diencephalon in the rabbit. I. An autoradiographic study of the efferent connections of the main and accessory olfactory bulbs. J. Comp. Neurol 163, 329–345. [PubMed: 1176643]

von Campenhausen H, and Mori K (2000). Convergence of segregated pheromonal pathways from the accessory olfactory bulb to the cortex in the mouse. Eur. J. Neurosci 12, 33–46. [PubMed: 10651858]

Chamero P, Marton TF, Logan DW, Flanagan K, Cruz JR, Saghatelian A, Cravatt BF, and Stowers L (2007). Identification of protein pheromones that promote aggressive behaviour. Nature 450, 899–902. [PubMed: 18064011]

Chen Y, Lin Y-C, Kuo T-W, and Knight ZA (2015). Sensory detection of food rapidly modulates arcuate feeding circuits. Cell 160, 829–841. [PubMed: 25703096]

Claro F, Segovia S, Guilamón A, and Del Abril A (1995). Lesions in the medial posterior region of the BST impair sexual behavior in sexually experienced and inexperienced male rats. Brain Res. Bull 36, 1–10. [PubMed: 7882041]

Connor J (1972). Olfactory control of aggressive and sexual behavior in the mouse (Mus musculus L.). Psychon Sci 27, 1–3.

Cooke BM, and Simerly RB (2005). Ontogeny of bidirectional connections between the medial nucleus of the amygdala and the principal bed nucleus of the stria terminalis in the rat. J. Comp. Neurol 489, 42–58. [PubMed: 15977169]

Crawley JN, Schleidt WM, and Contrera JF (1975). Does social environment decrease propensity to fight in male mice? Behavioral Biology 15, 73–83. [PubMed: 1237289]

Crestani CC, Alves FH, Gomes FV, Resstel LB, Correa FM, and Herman JP (2013). Mechanisms in the bed nucleus of the stria terminalis involved in control of autonomic and neuroendocrine functions: a review. Curr Neuropharmacol 11, 141–159. [PubMed: 23997750]

Cui G, Jun SB, Jin X, Pham MD, Vogel SS, Lovinger DM, and Costa RM (2013). Concurrent activation of striatal direct and indirect pathways during action initiation. Nature 494, 238–242. [PubMed: 23354054]

Davis BJ, Macrides F, Youngs WM, Schneider SP, and Rosene DL (1978). Efferents and centrifugal afferents of the main and accessory olfactory bulbs in the hamster. Brain Res. Bull 3, 59–72. [PubMed: 75756]

Dong H-W, and Swanson LW (2004). Projections from bed nuclei of the stria terminalis, posterior division: implications for cerebral hemisphere regulation of defensive and reproductive behaviors. J. Comp. Neurol 471, 396–433. [PubMed: 15022261]

Emery DE, and Sachs BD (1976). Copulatory behavior in male rats with lesions in the bed nucleus of the stria terminalis. Physiol. Behav 17, 803–806. [PubMed: 1026988]

Fenno L, Yizhar O, and Deisseroth K (2011). The development and application of optogenetics. Annu. Rev. Neurosci 34, 389–412. [PubMed: 21692661]

Ferrero DM, Lemon JK, Fluegge D, Pashkovski SL, Korzan WJ, Datta SR, Spehr M, Fendt M, and Liberles SD (2011). Detection and avoidance of a carnivore odor by prey. Proc. Natl. Acad. Sci. U.S.A 108, 11235–11240. [PubMed: 21690383]

Fisher CR, Graves KH, Parlow AF, and Simpson ER (1998). Characterization of mice deficient in aromatase (ArKO) because of targeted disruption of the cyp19 gene. Proc. Natl. Acad. Sci. U.S.A 95, 6965–6970. [PubMed: 9618522]

Fu X, Yan Y, Xu PS, Geerlof-Vidavsky I, Chong W, Gross ML, and Holy TE (2015). A Molecular Code for Identity in the Vomeronasal System. Cell 163, 313–323. [PubMed: 26435105]

Gammie SC, and Nelson RJ (2001). cFOS and pCREB activation and maternal aggression in mice. Brain Res 898, 232–241. [PubMed: 11306009]

Gandelman R (1972). Mice: postpartum aggression elicited by the presence of an intruder. Horm Behav 3, 23–28. [PubMed: 4681734]

Giardino WJ, Eban-Rothschild A, Christoffel DJ, Li S-B, Malenka RC, and de Lecea L (2018). Parallel circuits from the bed nuclei of stria terminalis to the lateral hypothalamus drive opposing emotional states. Nat. Neurosci 21, 1084–1095. [PubMed: 30038273]

Gu G, Cornea A, and Simerly RB (2003). Sexual differentiation of projections from the principal nucleus of the bed nuclei of the stria terminalis. J. Comp. Neurol 460, 542–562. [PubMed: 12717713]

Guillamón A, Segovia S, and del Abril A (1988). Early effects of gonadal steroids on the neuron number in the medial posterior region and the lateral division of the bed nucleus of the stria terminalis in the rat. Brain Res. Dev. Brain Res 44, 281–290. [PubMed: 3224428]

Gunaydin LA, Grosenick L, Finkelstein JC, Kauvar IV, Fenno LE, Adhikari A, Lammel S, Mirzabekov JJ, Airan RD, Zalocusky KA, et al. (2014). Natural neural projection dynamics underlying social behavior. Cell 157, 1535–1551. [PubMed: 24949967]

Haga-Yamanaka S, Ma L, He J, Qiu Q, Lavis LD, Looger LL, and Yu CR (2014). Integrated action of pheromone signals in promoting courtship behavior in male mice. Elife 3, e03025. [PubMed: 25073926]

Halem HA, Cherry JA, and Baum MJ (1999). Vomeronasal neuroepithelium and forebrain Fos responses to male pheromones in male and female mice. J. Neurobiol 39, 249–263. [PubMed: 10235679]

Hammen GF, Turaga D, Holy TE, and Meeks JP (2014). Functional organization of glomerular maps in the mouse accessory olfactory bulb. Nat. Neurosci 17, 953–961. [PubMed: 24880215]

Hashikawa K, Hashikawa Y, Tremblay R, Zhang J, Feng JE, Sabol A, Piper WT, Lee H, Rudy B, and Lin D (2017). Esr1+ cells in the ventromedial hypothalamus control female aggression. Nat. Neurosci 20, 1580–1590. [PubMed: 28920934]

He J, Ma L, Kim S, Nakai J, and Yu CR (2008). Encoding gender and individual information in the mouse vomeronasal organ. Science 320, 535–538. [PubMed: 18436787]

Holy TE (2018). The Accessory Olfactory System: Innately Specialized or Microcosm of Mammalian Circuitry? Annu. Rev. Neurosci 41, 501–525. [PubMed: 29727596]

Holy TE, Dulac C, and Meister M (2000). Responses of vomeronasal neurons to natural stimuli. Science 289, 1569–1572. [PubMed: 10968796]

Honda S, Harada N, Ito S, Takagi Y, and Maeda S (1998). Disruption of sexual behavior in male aromatase-deficient mice lacking exons 1 and 2 of the cyp19 gene. Biochem. Biophys. Res. Commun 252, 445–449. [PubMed: 9826549]

Hong W, Kim D-W, and Anderson DJ (2014). Antagonistic control of social versus repetitive self-grooming behaviors by separable amygdala neuronal subsets. Cell 158, 1348–1361. [PubMed: 25215491]

Isogai Y, Si S, Pont-Lezica L, Tan T, Kapoor V, Murthy VN, and Dulac C (2011). Molecular organization of vomeronasal chemoreception. Nature 478, 241–245. [PubMed: 21937988]

Kang N, Baum MJ, and Cherry JA (2009). A direct main olfactory bulb projection to the "vomeronasal" amygdala in female mice selectively responds to volatile pheromones from males. Eur. J. Neurosci 29, 624–634. [PubMed: 19187265]

Kang N, McCarthy EA, Cherry JA, and Baum MJ (2011a). A sex comparison of the anatomy and function of the main olfactory bulb-medial amygdala projection in mice. Neuroscience 172, 196–204. [PubMed: 21070839]

Kang N, Baum MJ, and Cherry JA (2011b). Different profiles of main and accessory olfactory bulb mitral/tufted cell projections revealed in mice using an anterograde tracer and a whole-mount, flattened cortex preparation. Chem. Senses 36, 251–260. [PubMed: 21177285]

Keller M, Baum MJ, Brock O, Brennan PA, and Bakker J (2009). The main and the accessory olfactory systems interact in the control of mate recognition and sexual behavior. Behav. Brain Res 200, 268–276. [PubMed: 19374011]

Kimoto H, Haga S, Sato K, and Touhara K (2005). Sex-specific peptides from exocrine glands stimulate mouse vomeronasal sensory neurons. Nature 437, 898–901. [PubMed: 16208374]

Kimoto H, Sato K, Nodari F, Haga S, Holy TE, and Touhara K (2007). Sex- and strain-specific expression and vomeronasal activity of mouse ESP family peptides. Curr. Biol 17, 1879–1884. [PubMed: 17935991]

King JA (1957). Relationships between early social experience and adult aggressive behavior in inbred mice. J Genet Psychol 90, 151–166. [PubMed: 13449290]

Lee H, Kim D-W, Remedios R, Anthony TE, Chang A, Madisen L, Zeng H, and Anderson DJ (2014). Scalable control of mounting and attack by Esr1+ neurons in the ventromedial hypothalamus. Nature 509, 627–632. [PubMed: 24739975]

Lehman MN, Powers JB, and Winans SS (1983). Stria terminalis lesions alter the temporal pattern of copulatory behavior in the male golden hamster. Behav. Brain Res 8, 109–128. [PubMed: 6849676]

Lephart ED (1996). A review of brain aromatase cytochrome P450. Brain Res. Brain Res. Rev 22, 1–26. [PubMed: 8871783]

Leypold BG, Yu CR, Leinders-Zufall T, Kim MM, Zufall F, and Axel R (2002). Altered sexual and social behaviors in trp2 mutant mice. Proc. Natl. Acad. Sci. U.S.A 99, 6376–6381. [PubMed: 11972034]

Li Y, Mathis A, Grewe BF, Osterhout JA, Ahanonu B, Schnitzer MJ, Murthy VN, and Dulac C (2017). Neuronal Representation of Social Information in the Medial Amygdala of Awake Behaving Mice. Cell 171, 1176–1190.e17. [PubMed: 29107332]

Liberles SD (2014). Mammalian pheromones. Annu. Rev. Physiol 76, 151–175. [PubMed: 23988175]

Liberles SD (2015). Trace amine-associated receptors: ligands, neural circuits, and behaviors. Curr. Opin. Neurobiol 34, 1–7. [PubMed: 25616211]

Liu YC, Salamone JD, and Sachs BD (1997). Lesions in medial preoptic area and bed nucleus of stria terminalis: differential effects on copulatory behavior and noncontact erection in male rats. J. Neurosci 17, 5245–5253. [PubMed: 9185562]

Luo M, Fee MS, and Katz LC (2003). Encoding pheromonal signals in the accessory olfactory bulb of behaving mice. Science 299, 1196–1201. [PubMed: 12595684]

Mandiyan VS, Coats JK, and Shah NM (2005). Deficits in sexual and aggressive behaviors in Cnga2 mutant mice. Nat. Neurosci 8, 1660–1662. [PubMed: 16261133]

Maruniak JA, Wysocki CJ, and Taylor JA (1986). Mediation of male mouse urine marking and aggression by the vomeronasal organ. Physiol. Behav 37, 655–657. [PubMed: 3749330]

Matsumoto T, Honda S, and Harada N (2003). Alteration in sex-specific behaviors in male mice lacking the aromatase gene. Neuroendocrinology 77, 416–424. [PubMed: 12845227]

McCarthy MM (2008). Estradiol and the developing brain. Physiol. Rev 88, 91–124. [PubMed: 18195084]

Meeks JP, Arnson HA, and Holy TE (2010). Representation and transformation of sensory information in the mouse accessory olfactory system. Nat. Neurosci 13, 723–730. [PubMed: 20453853]

Moga MM, Saper CB, and Gray TS (1989). Bed nucleus of the stria terminalis: cytoarchitecture, immunohistochemistry, and projection to the parabrachial nucleus in the rat. J. Comp. Neurol 283, 315–332. [PubMed: 2568370]

Morgan CW, Julien O, Unger EK, Shah NM, and Wells JA (2014). Turning on caspases with genetics and small molecules. Meth. Enzymol 544, 179–213. [PubMed: 24974291]

Naftolin F, Ryan KJ, and Petro Z (1971). Aromatization of androstenedione by limbic system tissue from human foetuses. J. Endocrinol 51, 795–796. [PubMed: 5138326]

Nassi JJ, and Callaway EM (2009). Parallel processing strategies of the primate visual system. Nat. Rev. Neurosci 10, 360–372. [PubMed: 19352403]

Nelson RJ, and Trainor BC (2007). Neural mechanisms of aggression. Nat. Rev. Neurosci 8, 536–546. [PubMed: 17585306]

Ng L, Bernard A, Lau C, Overly CC, Dong H-W, Kuan C, Pathak S, Sunkin SM, Dang C, Bohland JW, et al. (2009). An anatomic gene expression atlas of the adult mouse brain. Nat. Neurosci 12, 356–362. [PubMed: 19219037]

Nodari F, Hsu F-F, Fu X, Holekamp TF, Kao L-F, Turk J, and Holy TE (2008). Sulfated steroids as natural ligands of mouse pheromone-sensing neurons. J. Neurosci 28, 6407–6418. [PubMed: 18562612]

O'Connell RJ, and Meredith M (1984). Effects of volatile and nonvolatile chemical signals on male sex behaviors mediated by the main and accessory olfactory systems. Behav. Neurosci 98, 1083–1093. [PubMed: 6508913]

Omura M, and Mombaerts P (2014). Trpc2-expressing sensory neurons in the main olfactory epithelium of the mouse. Cell Rep 8, 583–595. [PubMed: 25001287]

Pankevich DE, Baum MJ, and Cherry JA (2004). Olfactory sex discrimination persists, whereas the preference for urinary odorants from estrous females disappears in male mice after vomeronasal organ removal. J. Neurosci 24, 9451–9457. [PubMed: 15496681]

Pankevich DE, Cherry JA, and Baum MJ (2006). Effect of vomeronasal organ removal from male mice on their preference for and neural Fos responses to female urinary odors. Behav. Neurosci 120, 925–936. [PubMed: 16893298]

Pfaus JG, and Heeb MM (1997). Implications of immediate-early gene induction in the brain following sexual stimulation of female and male rodents. Brain Res. Bull 44, 397–407. [PubMed: 9370204]

Powers JB, Newman SW, and Bergondy ML (1987). MPOA and BNST lesions in male Syrian hamsters: differential effects on copulatory and chemoinvestigatory behaviors. Behav. Brain Res 23, 181–195. [PubMed: 3555537]

Ramos SM, and DeBold JF (2000). Fos expression in female hamsters after various stimuli associated with mating. Physiol. Behav 70, 557–566. [PubMed: 11111011]

Remedios R, Kennedy A, Zelikowsky M, Grewe BF, Schnitzer MJ, and Anderson DJ (2017). Social behaviour shapes hypothalamic neural ensemble representations of conspecific sex. Nature 550, 388–392. [PubMed: 29052632]

Sam M, Vora S, Malnic B, Ma W, Novotny MV, and Buck LB (2001). Neuropharmacology: Odorants may arouse instinctive behaviours. Nature 412, 142–142. [PubMed: 11449261]

Scott JP (1966). Agonistic behavior of mice and rats: a review. Am. Zool 6, 683–701. [PubMed: 4859807]

Seabrook TA, Burbridge TJ, Crair MC, and Huberman AD (2017). Architecture, Function, and Assembly of the Mouse Visual System. Annu. Rev. Neurosci 40, 499–538. [PubMed: 28772103]

Segovia S, and Guillamón A (1993). Sexual dimorphism in the vomeronasal pathway and sex differences in reproductive behaviors. Brain Res. Brain Res. Rev 18, 51–74. [PubMed: 8467350]

Shah NM, Pisapia DJ, Maniatis S, Mendelsohn MM, Nemes A, and Axel R (2004). Visualizing sexual dimorphism in the brain. Neuron 43, 313–319. [PubMed: 15294140]

Simerly RB (2002). Wired for reproduction: organization and development of sexually dimorphic circuits in the mammalian forebrain. Annu. Rev. Neurosci 25, 507–536. [PubMed: 12052919]

Stack EC, Balakrishnan R, Numan MJ, and Numan M (2002). A functional neuroanatomical investigation of the role of the medial preoptic area in neural circuits regulating maternal behavior. Behav. Brain Res 131, 17–36. [PubMed: 11844569]

Sternson SM, and Roth BL (2014). Chemogenetic tools to interrogate brain functions. Annu. Rev. Neurosci 37, 387–407. [PubMed: 25002280]

Stowers L, Holy TE, Meister M, Dulac C, and Koentges G (2002). Loss of sex discrimination and male-male aggression in mice deficient for TRP2. Science 295, 1493–1500. [PubMed: 11823606]

Südhof TC (2015). Reproducibility: Experimental mismatch in neural circuits. Nature 528, 338–339. [PubMed: 26649825]

Swanson LW (2000). Cerebral hemisphere regulation of motivated behavior. Brain Res 886, 113–164. [PubMed: 11119693]

Takahashi A, and Miczek KA (2013). Neurogenetics of Aggressive Behavior: Studies in Rodents. Curr Top Behav Neurosci

Tamamaki N, Yanagawa Y, Tomioka R, Miyazaki J-I, Obata K, and Kaneko T (2003). Green fluorescent protein expression and colocalization with calretinin, parvalbumin, and somatostatin in the GAD67-GFP knock-in mouse. J. Comp. Neurol 467, 60–79. [PubMed: 14574680]

Thompson ML, and Edwards DA (1971). Experiential and strain determinants of the estrogen-progesterone induction of sexual receptivity in spayed female mice. Hormones and Behavior 2, 299–305.

Toda K, Saibara T, Okada T, Onishi S, and Shizuta Y (2001). A loss of aggressive behaviour and its reinstatement by oestrogen in mice lacking the aromatase gene (Cyp19). J. Endocrinol 168, 217–220. [PubMed: 11182758]

Tolokh II, Fu X, and Holy TE (2013). Reliable sex and strain discrimination in the mouse vomeronasal organ and accessory olfactory bulb. J. Neurosci 33, 13903–13913. [PubMed: 23966710]

Trinh K, and Storm DR (2003). Vomeronasal organ detects odorants in absence of signaling through main olfactory epithelium. Nat. Neurosci 6, 519–525. [PubMed: 12665798]

Unger EK, Burke KJ, Yang CF, Bender KJ, Fuller PM, and Shah NM (2015). Medial amygdalar aromatase neurons regulate aggression in both sexes. Cell Rep 10, 453–462. [PubMed: 25620703]

Valcourt RJ, and Sachs BD (1979). Penile reflexes and copulatory behavior in male rats following lesions in the bed nucleus of the stria terminalis. Brain Res. Bull 4, 131–133. [PubMed: 466486]

Vong L, Ye C, Yang Z, Choi B, Chua S, and Lowell BB (2011). Leptin action on GABAergic neurons prevents obesity and reduces inhibitory tone to POMC neurons. Neuron 71, 142–154. [PubMed: 21745644]

Walker DL, Toufexis DJ, and Davis M (2003). Role of the bed nucleus of the stria terminalis versus the amygdala in fear, stress, and anxiety. Eur. J. Pharmacol 463, 199–216. [PubMed: 12600711]

Wang Z, Sindreu CB, Li V, Nudelman A, Chan GC-K, and Storm DR (2006). Pheromone Detection in Male Mice Depends on Signaling through the Type 3 Adenylyl Cyclase in the Main Olfactory Epithelium. J. Neurosci 26, 7375–7379. [PubMed: 16837584]

Wei Y-C, Wang S-R, Jiao Z-L, Zhang W, Lin J-K, Li X-Y, Li S-S, Zhang X, and Xu X-H (2018). Medial preoptic area in mice is capable of mediating sexually dimorphic behaviors regardless of gender. Nat Commun 9, 279. [PubMed: 29348568]

Wersinger SR, Sannen K, Villalba C, Lubahn DB, Rissman EF, and De Vries GJ (1997). Masculine sexual behavior is disrupted in male and female mice lacking a functional estrogen receptor alpha gene. Horm Behav 32, 176–183. [PubMed: 9454668]

Wu MV, Manoli DS, Fraser EJ, Coats JK, Tollkuhn J, Honda S-I, Harada N, and Shah NM (2009). Estrogen masculinizes neural pathways and sex-specific behaviors. Cell 139, 61–72. [PubMed: 19804754]

Xu X, Coats JK, Yang CF, Wang A, Ahmed OM, Alvarado M, Izumi T, and Shah NM (2012). Modular genetic control of sexually dimorphic behaviors. Cell 148, 596–607. [PubMed: 22304924]

Yang CF, and Shah NM (2014). Representing sex in the brain, one module at a time. Neuron 82, 261–278. [PubMed: 24742456]

Yang CF, Chiang MC, Gray DC, Prabhakaran M, Alvarado M, Juntti SA, Unger EK, Wells JA, and Shah NM (2013). Sexually dimorphic neurons in the ventromedial hypothalamus govern mating in both sexes and aggression in males. Cell 153, 896–909. [PubMed: 23663785]

Yang T, Yang CF, Chizari MD, Maheswaranathan N, Burke KJ, Borius M, Inoue S, Chiang MC, Bender KJ, Ganguli S, et al. (2017). Social Control of Hypothalamus-Mediated Male Aggression. Neuron 95, 955–970.e4. [PubMed: 28757304]

Yao S, Bergan J, Lanjuin A, and Dulac C (2017). Oxytocin signaling in the medial amygdala is required for sex discrimination of social cues. Elife 6.

Yoon H, Enquist LW, and Dulac C (2005). Olfactory inputs to hypothalamic neurons controlling reproduction and fertility. Cell 123, 669–682. [PubMed: 16290037]

Zardetto-Smith AM, Beltz TG, and Johnson AK (1994). Role of the central nucleus of the amygdala and bed nucleus of the stria terminalis in experimentally-induced salt appetite. Brain Res 645, 123–134. [PubMed: 8062074]

Zhou JN, Hofman MA, Gooren LJ, and Swaab DF (1995). A sex difference in the human brain and its relation to transsexuality. Nature 378, 68–70. [PubMed: 7477289]

Highlights

- In sexually naïve males, activity of AB neurons encodes sex of conspecifics.
- Male AB neurons are required for sexual preference, mating, and aggression.
- Activation of male AB neurons promotes male-male sexual behavior.
- Females use other, non-AB neurons for sex recognition, mating, and maternal care.

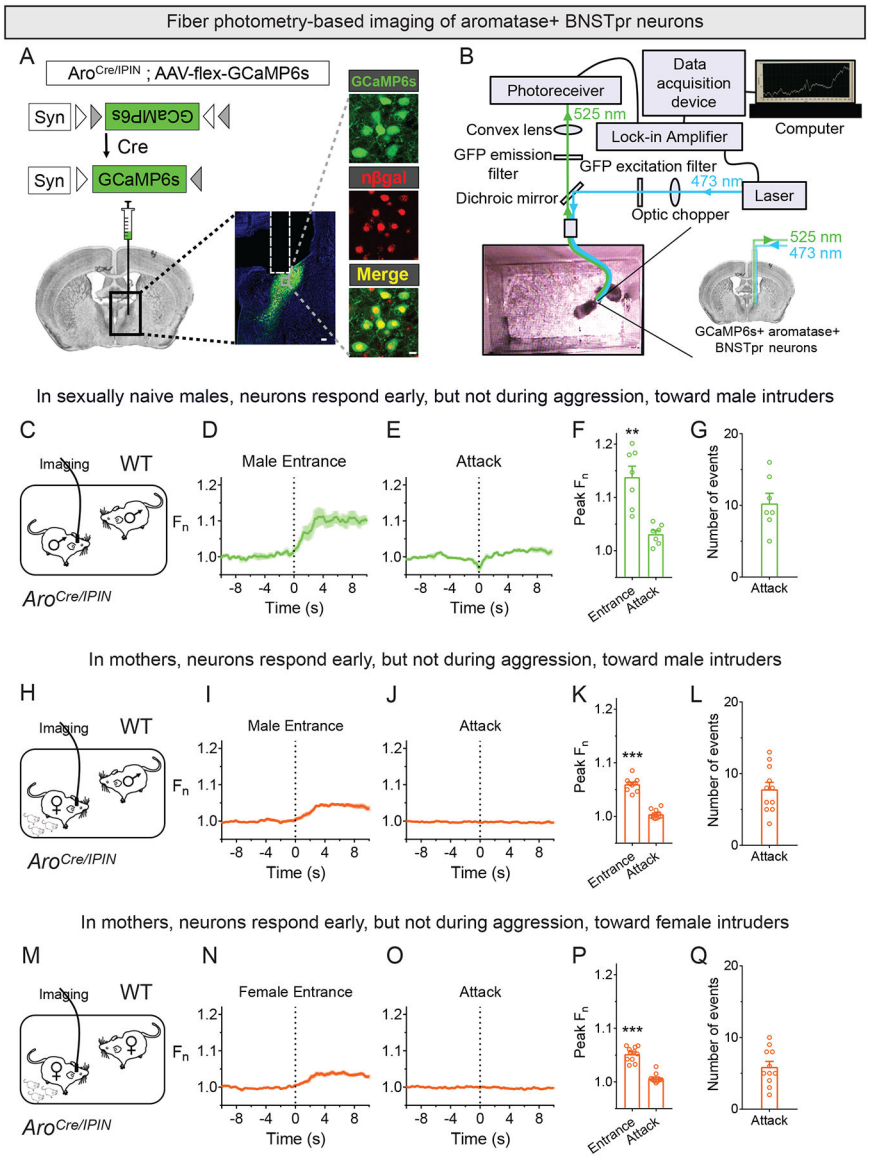

Figure 1: AB neurons are transiently activated in aggressive encounters

(A) Strategy to express GCaMP6s in AB neurons. Coronal section through adult male BNST (middle panel) expressing GCaMP6s and nuclear β-galactosidase (scale bar = 100 μm). Midline is on right, and tract of optic fiber implant is outlined dorsal to BNST. Insets show higher magnification of gray box in the middle panel (scale bar = 10 μm).

(B) Fiber photometry setup to image GCaMP6s in a freely behaving mouse.

(C-Q) Fiber photometry imaging of AB neurons in singly housed *Aro*$^{Cre/IPIN}$ male (C-G) or mother (H-Q) interacting with WT intruder for 15 min.

(C) A WT male is inserted into the cage of a sexually naïve male.

(D,E) Peri-event time plot (PETP) of GCaMP6s signal around entry of male and onset of attack episodes. For PETPs shown in this and other Figures, dark colored line and paler shaded region represent mean fluorescence and SEM, respectively. Vertical dashed black

line indicates beginning of event or behavior; Fn on y-axis of PETP represents fold change from baseline preceding the event.

(F) GCaMP6s signal increases upon entry of male. Peak Fn represents maximal fold change from baseline preceding the event. Tests of significance were performed, unless otherwise mentioned, by comparing peak Fn of various events to baseline GCaMP6s fluorescence preceding the event and correcting for multiple comparisons.

(G) Number of attacks by resident male.

(H) Male is inserted into the cage of a mother.

(I-K) GCaMP6s signal increases in mothers upon entry of male but not when she attacks him.

(L) Number of attacks by mothers.

(M) Female is inserted into the cage of a mother.

(N-P) GCaMP6s signal increases in mothers upon entry of female but not when she attacks her.

(Q) Number of attacks by mothers.

Mean ± SEM; hollow circles represent individual mice in these and subsequent figures. n = 7 (C-G), 11 (H-Q). **p<0.01, ***p<0.001. See also Figure S1, Table S1, and Movie S1.

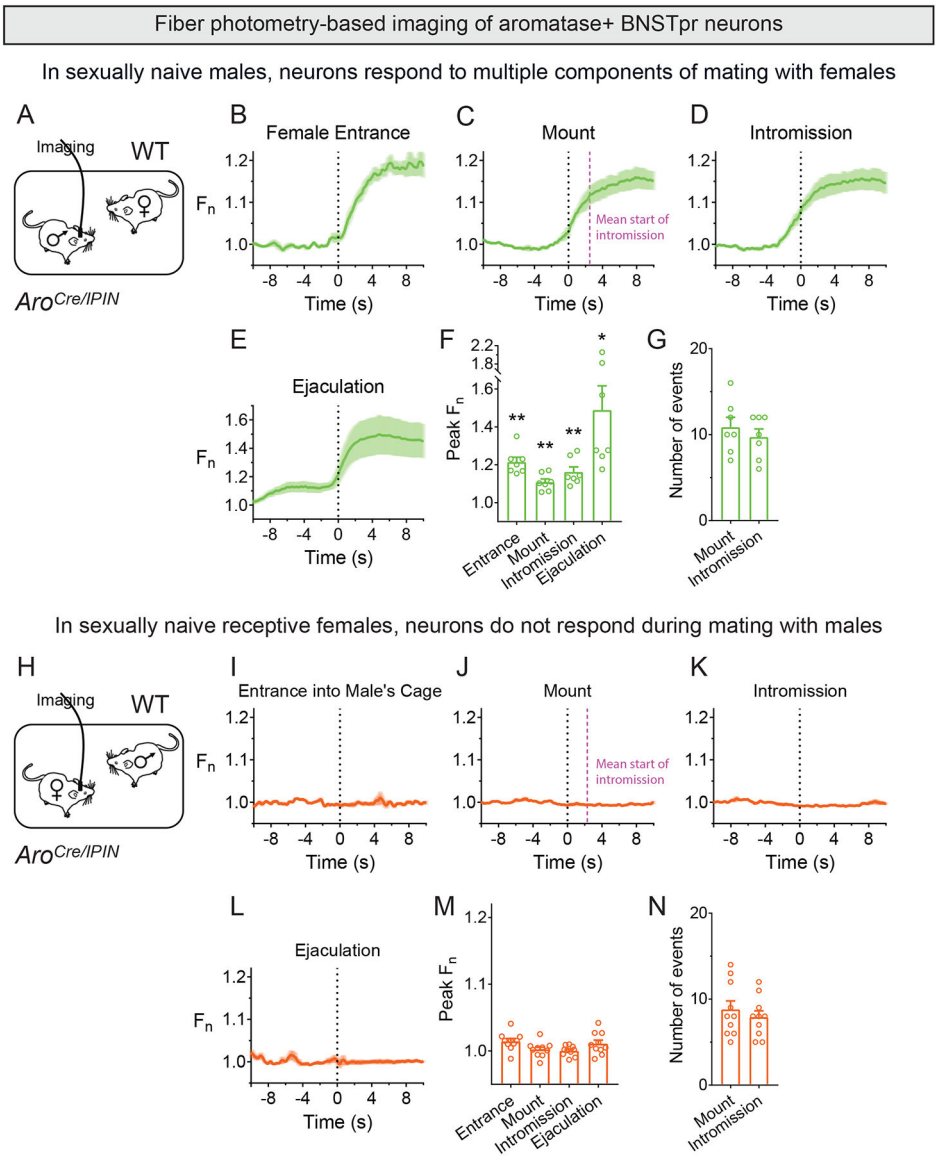

Figure 2: Male AB neurons are active during interactions with females

Fiber photometry imaging of AB neurons in sexually naive *Aro*$^{Cre/IPIN}$ males (A-G) or females (H-N) during 30 min test of mating behavior.

(A) Female is inserted into cage of a singly housed male.

(B-F) GCaMP6s signal increases upon entry of female, mounting, intromission, and ejaculation. Dashed pink line in (C) shows mean time at which mounting proceeded to intromission.

(G) Number of mount and intromission events displayed by each male.

(H) A receptive female is inserted into the cage of a WT male.

(I-M) No change in GCaMP6s signal following entry into the male's cage, mounting, intromission, and ejaculation.

(N) Number of mounts and intromissions by WT males toward *Aro*$^{Cre/IPIN}$ females.

Mean ± SEM. n = 7 (A-G), 10 (H-N). *p<0.05, **p<0.01. See also Figure S2, Table S1, and Movie S2.

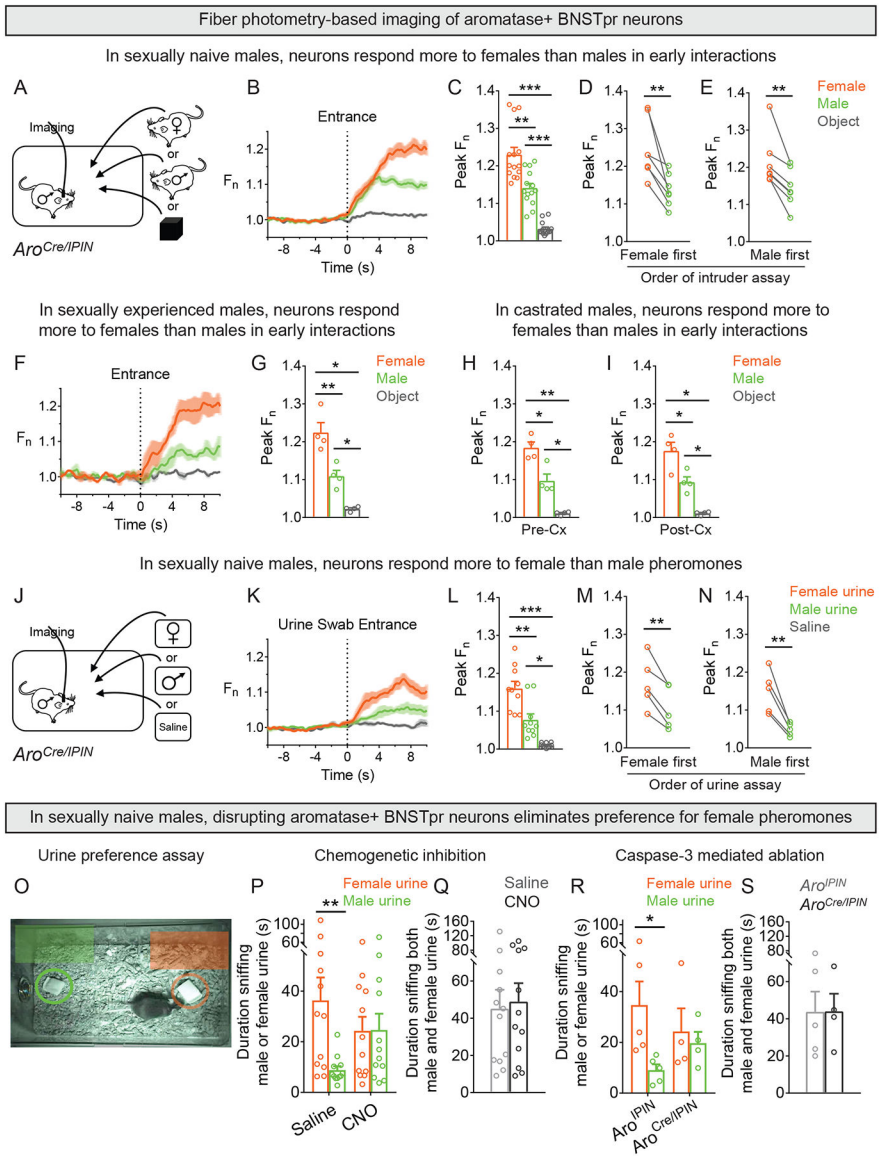

Figure 3: Male AB neurons respond differently to the two sexes and regulate sexual preference

(A-N) Fiber photometry of AB neurons in singly housed *Aro*$^{Cre/IPIN}$ male.

(A-I) A WT male, receptive female, or novel object was inserted for 3 min into the cage of a sexually naïve male.

(B,C) Larger change in activity of AB neurons upon entry of female compared to male. Males or females elicited larger response compared to object.

(D, E) AB neurons responded more to a female irrespective of whether they were exposed first to a female or male.

(F,G) Larger change in activity of AB neurons upon entry of female compared to male. Males and females elicited larger response compared to object.

(H,I) Larger change in activity of AB neurons in sexually naïve males prior to and after Cx upon entry of female compared to male. Males and females elicited larger response compared to object.

(J-N) A cotton swab wetted with female or male urine or saline was inserted for 3 min each into cage of a $Aro^{Cre/IPIN}$ male.

(K,L) AB neurons responded more to swab wetted with female compared to male urine. Urine wetted swabs elicited larger response compared to saline.

(M,N) Female urine elicited larger response irrespective of whether the male was exposed first to female or male urine.

(O-S) Cotton swabs wetted with male or female urine were simultaneously inserted into the cage of $Aro^{Cre/IPIN}$ males expressing DREADDi (O,P,Q) or engineered caspase-3 (O,R,S) to enable inhibition or ablation of AB neurons. Aro^{IPIN} males injected with caspase-3 payload served as controls (R,S).

(P) CNO eliminates preference for female urine.

(Q) Males given saline or CNO sniffed both swabs for similar total duration.

(R) Ablation of AB neurons eliminates preference for female urine.

(S) Both groups of males sniffed both swabs for similar total duration.

Mean ± SEM. n = 14 (A-E), 4 (F-I), 10 (J-N), 12 (P,Q), 5 (R,S, Aro^{IPIN}), 4 (R,S, $Aro^{Cre/IPIN}$). *p<0.05, **p<0.01, ***p<0.001. See also Figure S3, Table S1, and Movie S3.

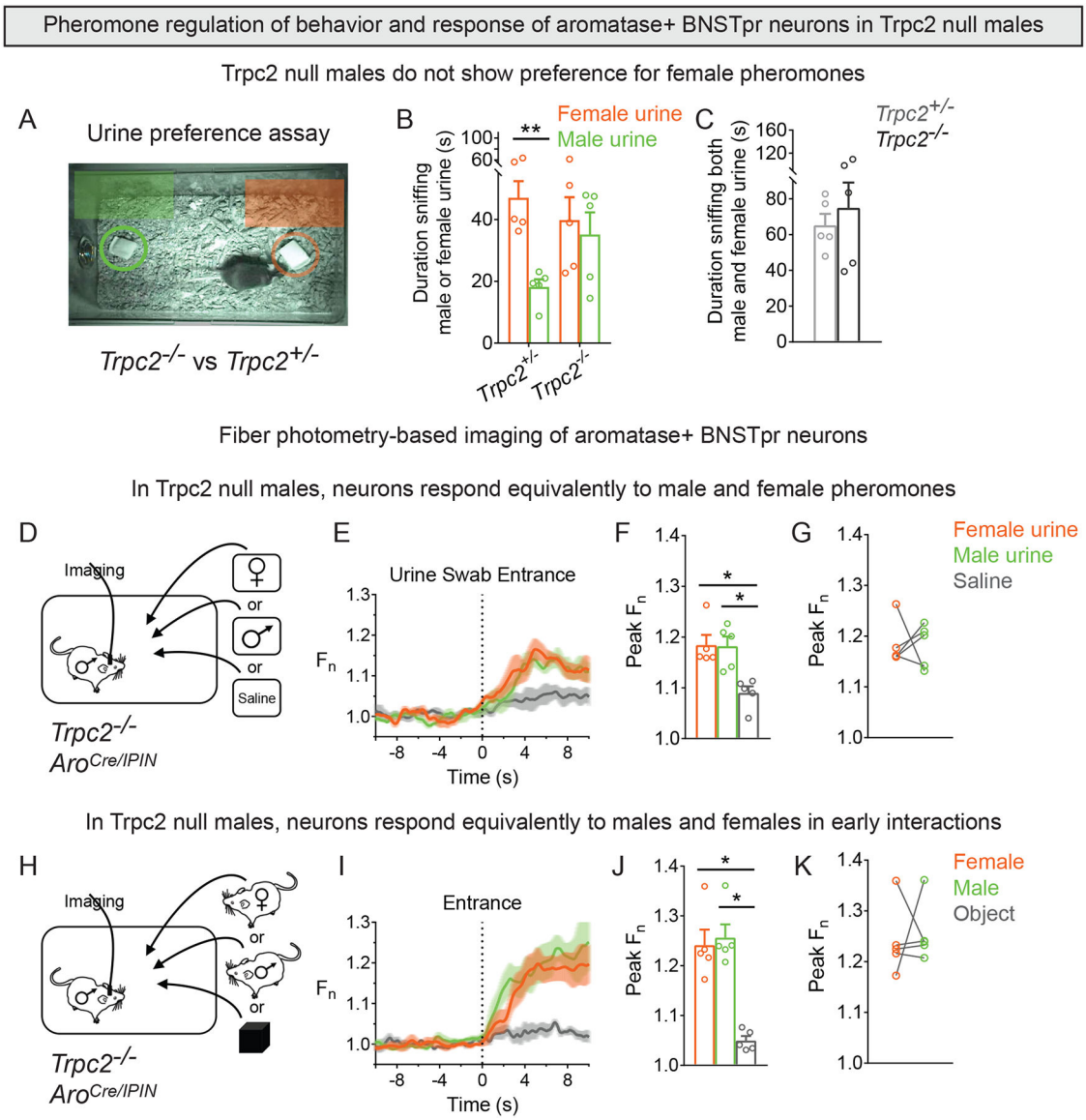

Figure 4: Sex-typical response of male AB neurons is dependent on pheromone sensing

(A-C) Sexually naïve *Trpc2*$^{-/-}$ and *Trpc2*$^{+/-}$ males were tested for urine preference.

(B) *Trpc2*$^{-/-}$ males sniff male and female urine equally.

(C) *Trpc2*$^{-/-}$ and *Trpc2*$^{+/-}$ males sniff male and female urine for similar total duration.

(D-K) Fiber photometry of AB neurons in singly housed males exposed to urine swab (D-G) or male, female, or novel object inserted into the cage for 3 min (H-K).

(D) A cotton swab wetted with female or male urine or saline was inserted into the cage.

(E,F) Response of AB neurons was similar to male or female urine and larger than that to saline.

(G) Similar response to male or female urine.

(H) A WT male, receptive female, or novel object was inserted into the cage.

(I,J) Response of AB neurons was similar to male or female intruder and larger than that to the object.

(K) Similar response to male or female intruder.

Mean ± SEM. n = 5 males/genotype. *p<0.05, **p<0.01. See also Figure S4 and Movie S4.

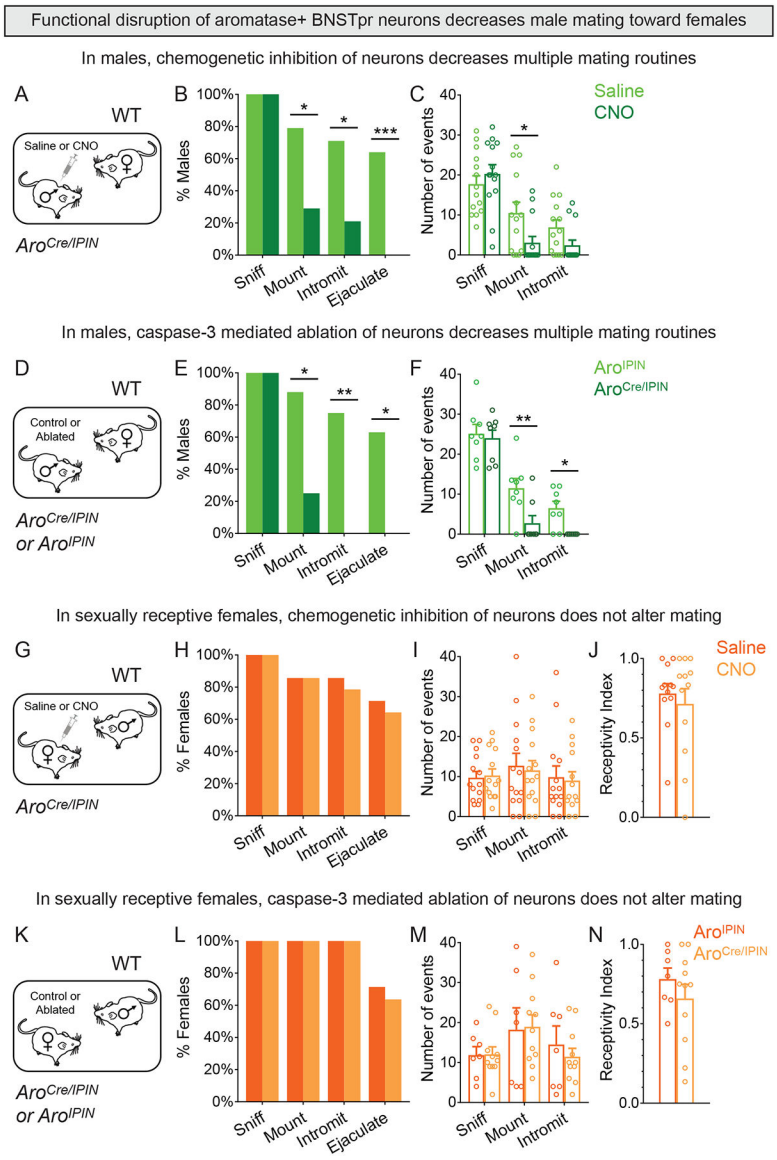

Figure 5: AB neurons play an essential role in male mating

(A-C) Behavior of singly housed male expressing DREADDi in AB neurons with receptive female intruder.

(B) CNO reduced percent males mounting or intromitting and eliminated ejaculation.

(C) CNO reduced mounts per assay.

(D-F) Behavior of singly housed males with caspase-3 targeted to AB neurons with receptive female intruder.

(E) Ablation of AB neurons reduced percent males mounting and precluded intromission or ejaculation.

(F) Ablation of AB neurons reduced mounts and intromissions per assay.

(G-J) Behavior of receptive female expressing DREADDi in AB neurons upon insertion into male cage.

(H-J) Behavior of females given CNO or saline is comparable.

(K-N) Behavior of receptive females with caspase-3 targeted to AB neurons upon insertion into male cage.

(L-N) Behavior of both groups of females is comparable.

Mean ± SEM. n = 14 (A-C), 8 (D-F, each genotype), 14 (G-J), 7 (K-N, Aro^{IPIN}) and 11 (K-N, $Aro^{Cre/IPIN}$). *p<0.05, **p<0.01, ***p<0.001. See also Figure S5, Table S1.

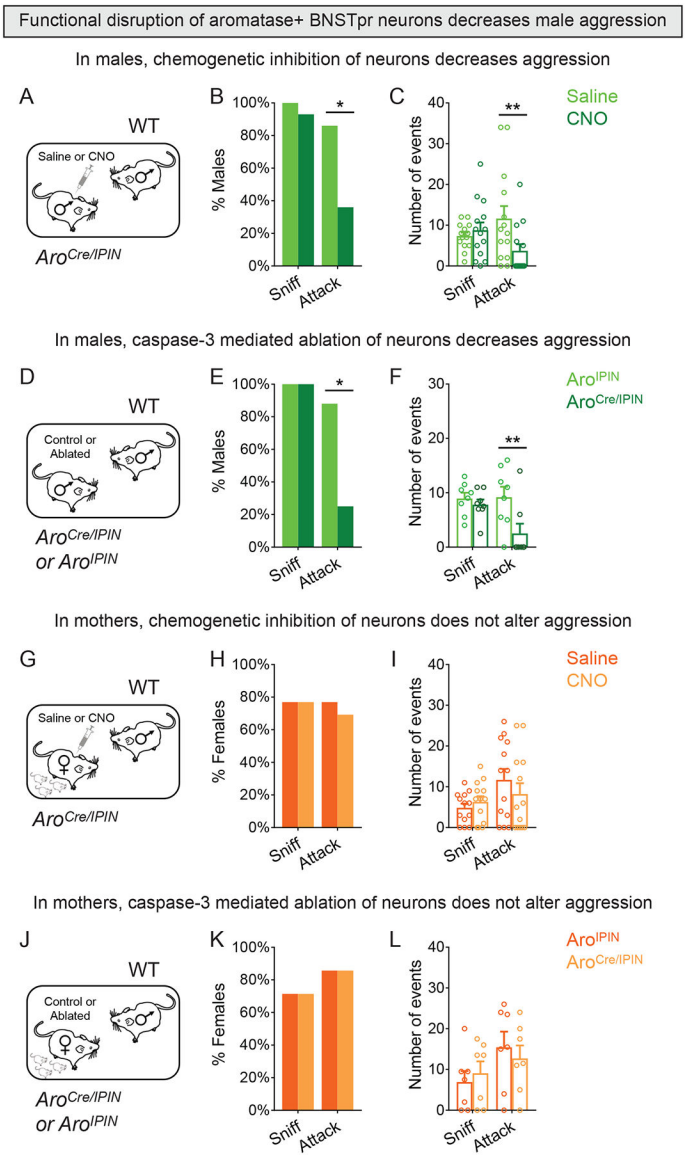

Figure 6: AB neurons play an essential role in male aggression

(A-C) Behavior of resident male expressing DREADDi in AB neurons with WT male intruder.

(B) CNO reduced percent residents attacking.

(C) CNO reduced attacks per assay.

(D-F) Behavior of resident males with caspase-3 targeted to AB neurons with WT male intruders.

(E) Ablation of AB neurons reduced percent residents attacking.

(F) Ablation of AB neurons reduced attacks per assay.

(G-I) Behavior of mothers expressing DREADDi in AB neurons with male intruder.

(H,I) Behavior of mothers given CNO or saline is comparable.

(J-L) Behavior of mothers with caspase-3 targeted to AB neurons with male intruder.

(K,L) Behavior of both groups of mothers is comparable.

Mean ± SEM. n = 14 (A-C), 8 (D-F, each genotype), 13 (G-I), 7 (J-L, each genotype). *p<0.05, **p<0.01. See also Figure S6, Table S1.

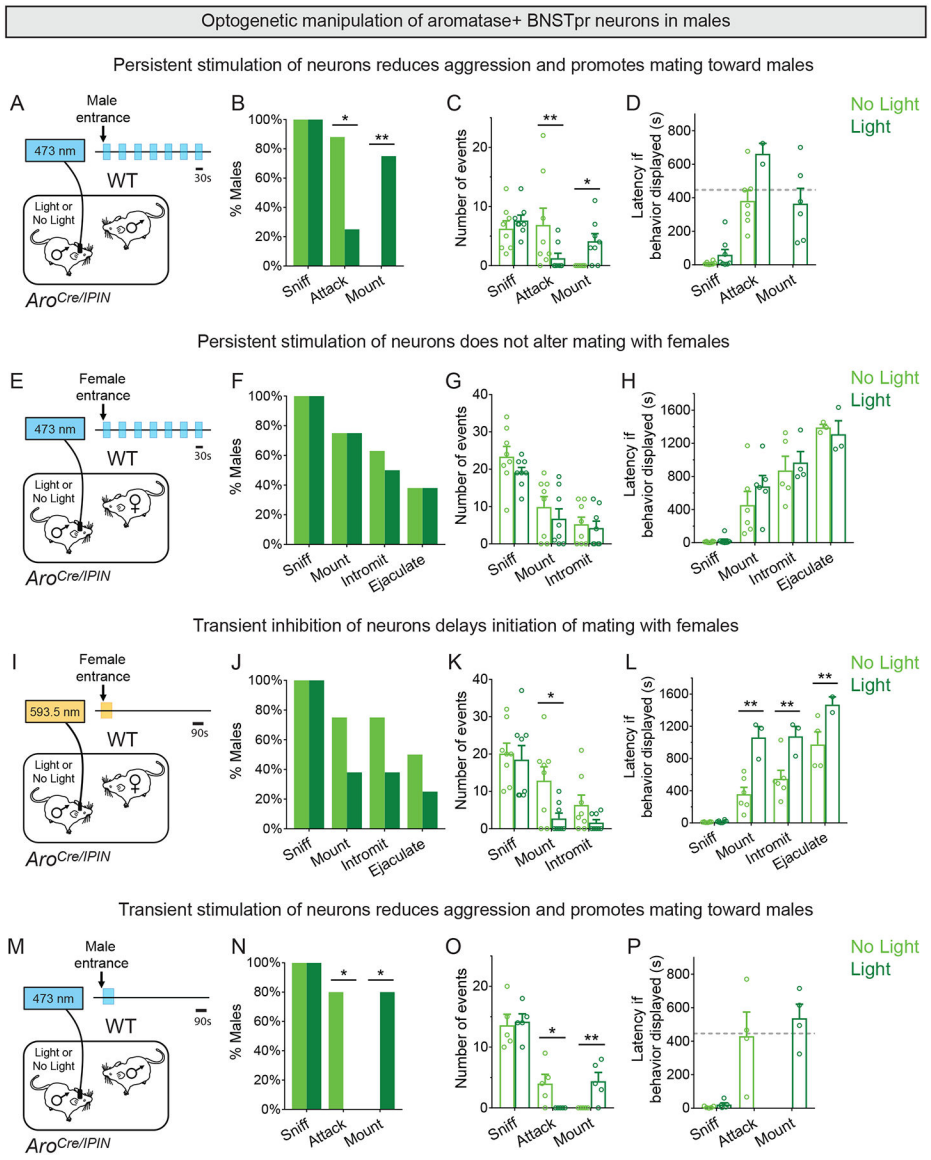

Figure 7: Early activity in male AB neurons promotes mating and inhibits fighting

(A-D) Laser illumination of ChR2+ AB neurons in resident males interacting with WT intruder male for 15 min.

(B) Laser illumination reduces probability of attacks and increases that of mounts toward the intruder.

(C) Laser illumination reduces attacks and increases mounts toward the intruder per assay.

(D) Latency to mount male intruder is similar to latency to mount receptive female intruder (shown by horizontal dashed line). Data for males mating with females is from panel H.

(E-H) Laser illumination of ChR2+ AB neurons in resident males interacting with receptive female intruder for 30 min.

(F-H) Laser illumination does not alter mating with females.

(I-L) Brief (90s) laser illumination of eNpHR3.0+ AB neurons in resident males interacting with receptive female intruders for 30 min.

(J) No significant change in percent males mating with optogenetic inhibition of AB neurons.
(K,L) Optogenetic inhibition of AB neurons reduces mounts per assay and increases latency to mount, intromit, and ejaculate.
(M-P) Brief (90s) laser illumination of ChR2+ AB neurons in resident males interacting with WT intruder males for 15 min.
(N) Laser illumination eliminates attacks and promotes mounting.
(O) Laser illumination reduces attacks and increases mounts per assay.
(P) Latency to mount intruder male is similar to latency to mount receptive female intruder (shown by horizontal dashed line). Data for males mating with females is from panel H. Mean ± SEM. n = 8 (A-H), 8 (I-L), 5 (M-P). *p<0.05, **p<0.01. See also Figure S7 and Movie S7.

KEY RESOURCES TABLE

REAGENT or RESOURCE	SOURCE	IDENTIFIER
Antibodies		
Sheep anti-GFP	Biorad	Cat # 4745-1051; RRID: AB_619712
Rat anti-RFP	Chromotek	Cat # 5f8-100; RRID: AB_2336064
Chicken anti-β-galactosidase	Abcam	Cat # 9361; RRID: AB_307210
Rabbit anti-Fos	EMD Millipore	Cat # PC38; RRID: AB_2106755
Donkey anti-sheep, Alexa 488 conjugate	Jackson ImmunoResearch	Cat # 713-545-147; RRID: AB_2340745
Donkey anti-rat, Cy3 conjugate	Jackson ImmunoResearch	Cat # 712-165-150; RRID: AB_2340666
Donkey anti-chicken, Alexa 488 conjugate	Jackson ImmunoResearch	Cat # 703-545-155; RRID: AB_2340375
Donkey anti-chicken, Cy3 conjugate	Jackson ImmunoResearch	Cat # 703-165-155; RRID: AB_2340363
Donkey anti-chicken, Alexa 647 conjugate	Jackson ImmunoResearch	Cat # 703-605-155; RRID: AB_2340379
Donkey anti-rabbit, Cy3 conjugate	Jackson ImmunoResearch	Cat # 711-165-152; RRID: AB_2307443
Bacterial and Virus Strains		
Recombinant adeno-associated virus: AAV1-Syn-flex-GCaMP6s	Penn Vector Core	Addgene number: 100845
Recombinant adeno-associated virus: AAV1-EF1α-flex-hChR2(H134R):eYFP	Penn Vector Core	Addgene number: 20298
Recombinant adeno-associated virus: AAV1-EF1α-flex-eNpHR3.0:eYFP	Penn Vector Core	Addgene number: 26966
Recombinant adeno-associated virus: AAV1-CAG-flex-eGFP	Penn Vector Core	Addgene number: 59331
Recombinant adeno-associated virus: AAV1-EF1α-taCasp3-TEVp	UNC Vector Core	Addgene number: 45580
Recombinant adeno-associated virus: AAV1-EF1α-flex-hM4DGi:mCherry	UNC Vector Core	Addgene number: 50461
Recombinant adeno-associated virus: AAV5-EF1α-flex-mCherry	UNC Vector Core	Addgene number: 50462
Recombinant adeno-associated virus: AAV1-EF1α-flex-eYFP	UNC Vector Core	Addgene number: 27056
Chemicals, Peptides, and Recombinant Proteins		
DAPI	Sigma-Aldrich	Cat # D9542; CAS 28718-90-3
Clozapine-N-oxide (CNO)	Enzo Life Sciences	Cat # BML-NS105-0005
Estradiol	Sigma-Aldrich	Cat # E8875;CAS 50-28-2
Progesterone	Sigma-Aldrich	Cat # P0130; CAS 57-83-0
2-phenylethylamine (PEA)	Sigma-Aldrich	Cat # 128945; CAS 64-04-0
Cadaverine	Sigma-Aldrich	Cat # D22606; CAS 462-94-2
Critical Commercial Assays		
Testosterone ELISA kit	Cayman	Cat # 582701
Experimental Models: Organisms/Strains		
Mouse: C57BL/6J	The Jackson Laboratory	Cat # 000664; RRID: IMSR_JAX:000664
Mouse: C57BL/6N	Charles River	Cat # 027
Mouse: Swiss Webster	Charles River	Cat # 024

REAGENT or RESOURCE	SOURCE	IDENTIFIER
Mouse: 129/SvEvTac	Taconic Biosciences	Cat # 129SVE-M
Mouse: *Aro*^{Cre}	Unger et al., 2015	Cat # 027038; RRID: IMSR_JAX:027038
Mouse: *Aro*^{IPIN}	Wu et al., 2009	Cat # 012377; RRID: IMSR_JAX:012377
Mouse: *Trpc2*$^{-/-}$	Leypold et al., 2002	N/A
Mouse: *Vgat*^{Cre}	Vong et al., 2011	Cat # 028862; RRID: IMSR_JAX:028862
Mouse: *Gad1*^{EGFP}	Tamamaki et al., 2003	N/A
Software and Algorithms		
ImageJ	NIH	https://imagej.nih.gov/ij/index.html; RRID: SCR_003070
MATLAB	MathWorks	https://www.mathworks.com/products.html; RRID: SCR_001622
GraphPad Prism 6	GraphPad Software	https://www.graphpad.com/scientificsoftware/prism/; RRID: SCR_002798